Tunable spin/charge Kondo effect at a double superconducting island connected to two spinless quantum wires

Domenico Giuliano,[1,2] Luca Lepori,[1,3] and Andrea Nava[1,4]

[1]*Dipartimento di Fisica, Università della Calabria Arcavacata di Rende I-87036, Cosenza, Italy*
[2]*I.N.F.N., Gruppo collegato di Cosenza, Arcavacata di Rende I-87036, Cosenza, Italy*
[3]*Istituto Italiano di Tecnologia, Graphene Labs, Via Morego 30, I-16163 Genova, Italy*
[4]*International School for Advanced Studies (SISSA), Via Bonomea 265, I-34136 Trieste, Italy*

(Received 20 November 2019; revised manuscript received 6 May 2020; accepted 7 May 2020; published 22 May 2020)

We propose that a pertinently engineered double superconducting island connected to two spinless one-dimensional conducting leads can work as a tunable (iso)spin Kondo and charge Kondo system, with the lead index regarded as an effective isospin degree of freedom. We evidence how, by tuning a single gate voltage applied to the island, it is possible to make the system switch from the (iso)spin Kondo to the charge Kondo phase, passing across an intermediate phase, in which the Kondo impurity is effectively irrelevant for the low-temperature behavior of the system. Eventually, we evidence how to probe the various phases by measuring the ac conductance tensor of our system, by emphasizing the features that should allow to identify the onset of the so far quite elusive "charge-2" charge Kondo effect.

DOI: 10.1103/PhysRevB.101.195140

I. INTRODUCTION

The Kondo effect has been experimentally seen for the first time as an upturn in the resistivity of metals doped with magnetic impurities, as the temperature T goes below the nonuniversal Kondo temperature T_K, typically of the order of a few Kelvin, or less [1,2]. On the theoretical side, the Kondo effect was readily explained in terms of a dynamical screening of the single-impurity magnetic moment by means of the spin density of itinerant electrons in the metal [1,2]. As $T \to 0$, the impurity moment is fully screened, which allows for trading the impurity for a local (Kondo) spin singlet, acting as a scattering center that forbids electrons from accessing the impurity site [2,3]. The Kondo spin singlet provides one of the few theoretically well-understood examples of strongly correlated states of matter. For this reason, soon after its discovery and its theoretical explanation, Kondo effect began to be used as a paradigmatic test bed for a number of remarkable analytical, as well as numerical, methods to study strongly correlated systems, including the well-celebrated Wilson's numerical renormalization group (RG) technique [4,5]. On top of that, it has been found how a peculiar realization of the effect, such as the "overscreened" one, in which more than one itinerant electron "channel" contributes to screen the magnetic impurity, yields to a novel phase of matter, which, differently from the local spin singlet, cannot be described within the "standard" Landau's Fermi-liquid framework [6].

Recently, a renewed interest has arisen in the Kondo effect [7], due to the possibility of realizing it in a controlled way in mesoscopic systems with tunable parameters, such as semiconducting quantum dots with metallic leads [8–11], in which Kondo effect is expected to appear as an upturn of the conductance, rather than of the resistivity, across the dot connected to the leads, or with superconducting leads [12–14], in which Kondo effect should be evidenced by a change in the behavior of the subgap (Josephson) supercurrent across the dot, when the leads are held at a fixed phase difference φ. In addition, since the effect is merely due to spin dynamics, it has been proposed that a "spin Kondo" effect can take place in systems with itinerant, low-energy excitations carrying spin, but not charge, such as XXZ spin-$\frac{1}{2}$ chains [15–17], which can be for instance realized by loading cold atoms on a pertinently designed optical lattice [18,19], or frustrated J_1-J_2 spin chains with J_2/J_1 tuned at the "critical" value at the phase transition between the spin liquid and the dimerized phase of the system [20]. In fact, realizations of the spin Kondo effect have recently been proposed at junctions of quantum spin chains [21–24], or of one-dimensional arrays of Josephson junctions [25–27]. Finally, it is worth mentioning the possibility, that has been recently put forward, that a remarkable "topological" Kondo effect might arise, in which the impurity spin is realized by means of Majorana modes emerging at the interface between topological superconductors and normal conductors (or the empty space) [28–30] and, more generally, the striking similarity between the Kondo physics and the hybridization between a Majorana mode and the itinerant electrons in a metal connected to the topological superconductor [31].

A key point about Kondo effect is that, aside from all the spin dynamics underneath, in order for the effect to take place, one generally needs an impurity with a twofold-degenerate ground state, which is able to switch from one state to the other via quantum number exchange processes with itinerant particles from the medium into which the impurity is embedded. In this respect, a number of proposals have been put forward in which Kondo effect is associated to *charge* rather than to spin degeneracy in the impurity ground state.

Such a charge-based version of Kondo effect is typically dubbed "charge Kondo" (CK) effect, to distinguish it from the "standard" "spin Kondo" (SK) effect. The CK effect was originally proposed as a possible mechanism, related to the "negative-U" Anderson model, able to induce a charge-dual version of the highly correlated, heavy-fermion ground state [32]. The CK effect has later on been theoretically studied in dots connected to bulk leads [33], in single-electron transistors [34–36], as well as in generalizations of the negative-U Anderson model [37–39], also involving optical lattice systems [40]. Overall, there are two main different realizations of CK effect. The former one does not require superconducting correlations. It consists in realizing the two degenerate impurity states at a quantum point contact with a finite charging energy tuned, by means of an external gate voltage, nearby the degeneracy point between two states differing by a single-electron charge e ("charge-1" CK). This proposal has been theoretically put forward in, e.g., Refs. [33–36,41] and eventually led to the experimental observation of the effect, discussed in Ref. [42]. At variance, a different realization of CK effect, in which the degenerate impurity states differ by a charge $2e$ ("charge-2" CK), has been proposed in, e.g., Refs. [32,37–39] (a detailed discussion about the two different realizations of CK is provided in, e.g., Ref. [43]).

Notwithstanding the great interest in CK effect, witnessed by the large number of papers on the topic, a clear-cut experimental verification of charge-2 CK effect is still lacking (differently from what happens for SK and for charge-1 CK effect). For this reason, in the last years there has been an increasing interest in realizing CK effect in a controlled way, in systems with tunable parameters. For instance, it has been proposed to realize CK effect in mesoscopic superconductors coupled to normal metals [43], in negative-U quantum dots with superconducting electrodes [44], and even in double quantum dot, in which the effect should be mediated by the Coulomb repulsion between the electrons at the double dot [45]. In general, defining an appropriate tunable device to probe CK effect, possibly in comparison with the more "standard" SK effect, is still an open challenge, also in view of the potential relevance of CK effect to explain the physics of, e.g., superconductivity in PbTe doped with Tl [38], or of impurities formed at dots in $LaSrO_3/SrTiO_3$ interfaces [46].

In this paper, we propose to realize charge-2 CK effect at a "minimal" tunable device in which one may in principle switch from SK to CK effect by just acting onto a limited number of system parameters (ideally, one parameter only). Our system, which we sketch in Fig. 1 in its "minimal" version, consists of two spinless conducting fermionic channels (the "leads"), connected to a "tunable" effective Kondo impurity K. In particular, we propose to realize the tunable Kondo impurity by means of a pertinently designed double superconducting island hosting four Majorana modes emerging at the end points of two spinless quantum wires deposited on top of it (see Fig. 2 for a sketch of the setup). Aside from technical details related to the design of our system, it is based on by now well-established features concerning the interplay between emerging Majorana fermion in condensed matter systems and the Kondo effect, a sample of which can be found in, e.g., Refs. [28–30,47–49]. In principle, our device can be experimentally realized similarly to setups already employed

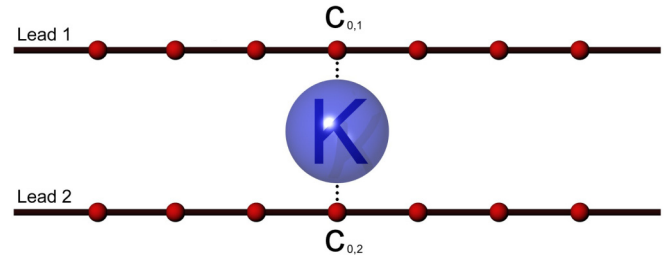

FIG. 1. Sketch of our proposed system: the two quantum wires are represented as one-dimensional lattices, while the tunable Kondo impurity is realized by connecting the leads to a double superconducting island with pertinently chosen parameters (see the main text).

to test the existence of Majorana modes [50–52] making use of, e.g., heterostructures of semiconductors coupled to s-wave superconductors [53] or linear junctions between superconductors and topological insulators [54]. To define an effective spin index, we regard the lead index of lead electrons as an effective isospin index. Yet, to ease the presentation, in the paper we refer to the effective isospin degree of freedom simply as lead electron spin. Doing so, we show that the Kondo-type coupling of K to lead electrons can be either SK like, or CK like, depending on the specific values of the tuning parameters.

Our design allows for changing in a controlled way the magnitude and the sign of the electronic interaction at the superconducting island. In the language of the Anderson impurity model Hamiltonian, which provides a reliable low-energy description of the island, this corresponds to tuning the system across a transition from the positive-U to the negative-U regime. For both signs of U the island ground state keeps twofold degenerate, thus triggering the onset of Kondo physics when connected to the leads. However, the nature of the degenerate ground-state doublet strongly depends on the sign of U. Eventually, this implies a transition from the SK to the CK regime at the change in the sign of the electronic interaction strength [45].

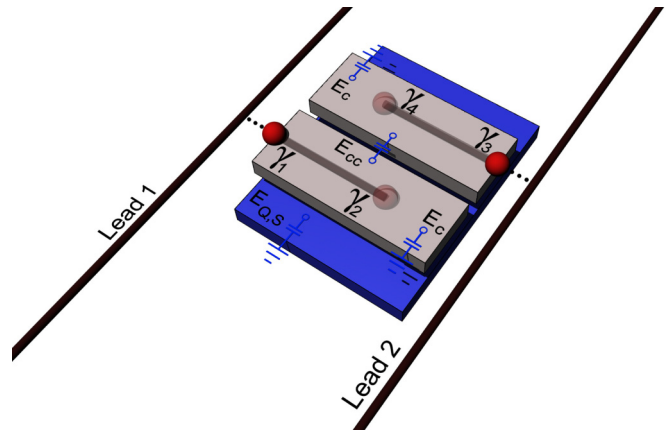

FIG. 2. Our proposed system: a couple of interacting spinless quantum wires are deposited on a double topological island, hosting four Majorana fermions. The Majorana fermions γ_1 and γ_3 are tunnel coupled to leads 1 and 2, respectively, as highlighted by the dashed lines in the figure.

Within our device, the SK and CK phases do not overlap in parameter space with each other. This avoids the simultaneous presence of both effects which, though making the physical scenario richer, does not possibly allow for a clear-cut detection of the latter effect against the former one [55]. In fact, the separate detection of either effect is even more favored by the fact that the SK and CK phases are separated, in parameter space, by an intermediate, "disconnected lead" phase, in which the impurity plays no relevant role for the low-T physics of the system.

To probe the various phases of our system, we propose to look at the ac conductance *across* the impurity, both over the same lead ("intralead"), as well as between different leads ("interlead"). Eventually, we show how a synoptic comparison of the intralead and of the interlead ac conductances offers a simple, though effective, way of detecting the SK and CK effects in our system. Moreover, when tuned within the CK phase, the Kondo impurity triggers off-diagonal conduction via a peculiar realization of crossed Andreev reflection between the two leads. In analogy to the devices discussed in Refs. [56,57], this suggests that, in a "dual" setup, in which a Cooper pair is injected into the leads through the impurity, our system might effectively work as a "long-distance electronic entangler", with potential applications to realizing large-distance entangled two-particle states.

The paper is organized as follows:

(i) In Sec. II, we introduce the lattice model Hamiltonian for our system. In particular, we discuss in detail how to engineer the double superconducting island at the center of the system, so to make it work as a spin Kondo or charge Kondo impurity, by acting onto a pertinent tuning parameter.

(ii) In Sec. III, we derive the effective low-energy, long-wavelength, continuum Hamiltonian description of our system in its various phases: the spin Kondo phase, the charge Kondo phase, and the decoupled lead phase.

(iii) In Sec. IV, we resort to a perturbative renormalization group analysis, to recover how the system scales with a running scale D [which we identify with either the (Boltzmann constant k times the) temperature T, or with the frequency of the ac applied voltage ω, depending on which scale is larger] toward the fixed point corresponding to each one of its phases.

(iv) In Sec. V, we discuss the dependence on ω of the intrawire and of the interwire ac conductance in each phase, focusing onto the low-temperature regime $\omega, kT_K \gg T$ and paying particular attention to the onset of the nonperturbative Kondo regime in the SK and CK phases. Eventually, we highlight how an appropriate measurement of the ac conductances as a function of ω and of the system parameters provides an effective means to map out the phase diagram of our system.

(v) In Sec. VI, we summarize our result by also discussing about a possible practical realization of our system and by eventually highlighting possible further developments of our work.

(vi) In the various appendices, we report the mathematical details of our derivation.

II. MODEL HAMILTONIAN

Our device is sketched in Fig. 1. To model it, we resort to a lattice Hamiltonian for two leads, which we represent as two $(2\ell+1)$-site chains, with ℓ eventually sent to ∞. The lattice Hamiltonian for the leads, $H_{0,\mathrm{Lat}}$, is given by

$$H_{0,\mathrm{Lat}} = \sum_{a=1,2} \left\{ -J_a \sum_{j=-\ell}^{\ell-1} [c^\dagger_{j,a} c_{j+1,a} + c^\dagger_{j+1,a} c_{j,a}] - \mu_a \sum_{j=-\ell}^{\ell} c^\dagger_{j,a} c_{j,a} \right\}, \tag{1}$$

with $\{c_{j,a}, c^\dagger_{j,a}\}$ being single-fermion annihilation/creation operators at site j of lead a, obeying the standard anticommutation relations $\{c_{j,a}, c^\dagger_{j',a'}\} = \delta_{j,j'}\delta_{a,a'}$. J_a and μ_a, respectively, correspond to the single-fermion hopping strength and to the onsite chemical potential in lead a. For the sake of simplicity, in the following we choose the parameters entering Eq. (1) independent of a. In fact, this only quantitatively affects the final result and, in any case, one may readily discuss the case of different parameters in the two leads by using the approach discussed in, e.g., Ref. [58] in the general case of a ladder of interacting quantum wires.

We now show how it is possible to realize a tunable Kondo Hamiltonian by connecting the two-leg ladder to a double superconducting island (DSI), with pertinently chosen parameters. Specifically, we consider an adapted version of the topological Kondo Hamiltonian introduced in Ref. [59], and then widely studied in Refs. [28–30,47,49,60–63]. In Fig. 2 we draw a sketch of the proposed device. It consists of two mesoscopic s-wave superconducting islands with two spinless quantum wires deposited onto each of them. According to Refs. [64,65], we expect four localized real Majorana modes to emerge at the end points of the wires. Let γ_1, γ_2 and γ_3, γ_4 be the two Majorana modes arising at wire 1 and 2, respectively. To construct the tunable Kondo Hamiltonian, we assume that γ_1 and γ_3 are tunnel coupled to, respectively, lead 1 and lead 2. Also, we assume that the length of each wire deposited on the islands and the distance between the wires are large enough to suppress the direct tunneling between the two Majorana modes at each wire. Yet, the two Majorana modes at the same island are assumed to be coupled to each other via the capacitive charging energy between each island and the ground. Finally, we assume a nonzero direct cross-capacitance coupling between the two superconducting islands and a Josephson coupling allowing for Cooper pair exchange between the islands and an underneath superconducting island S. As a result, the total Hamiltonian for the double-island system is given by

$$H_{\mathrm{Island}} = H_{I,1} + H_{I,2} + H_C + H_S. \tag{2}$$

In Eq. (2), $H_{I,1}$ and $H_{I,2}$ describe the two islands coupled to S. They are defined so that

$$H_{I,1} + H_{I,2} = -E_J \cos(\chi_1) + E_C[2N_1 + n_1 - Q_1]^2 - E_J \cos(\chi_2) + E_C[2N_2 + n_2 - Q_2]^2, \tag{3}$$

with $n_i = \frac{1}{2}[1 + i\gamma_{2i-1}\gamma_{2i}]$, so that $2N_i + n_i$ is the total charge (in units of e) lying at island i, including a possible quasiparticle occupying the Dirac level made out of the two Majorana modes, and with Q_i being the back-gate voltage, determined by the voltage across the capacitor. E_C is the charging energy

of each island, and $-E_J\cos(\chi_i)$ corresponds to the Josephson coupling between island i and the superconductor underneath, with the phase difference χ_i canonically conjugate to the number of Cooper pairs (N_i).

H_C in Eq. (2) describes the cross-capacitive coupling between the two islands. It is given by

$$H_C = E_{CC}[2N_1 + n_1 - Q_1][2N_2 + n_2 - Q_2], \tag{4}$$

with E_{CC} being the cross-charging energy. Finally, H_S describes the superconducting island S, which we assume to be large enough for it to be able to absorb/emit Cooper pair at no additional cost of energy. The charging energies of each island and the cross-charging energy are obtained from the inverse of the Maxwell capacitance matrix $\mathbf{C}$, that for the system described above reads as

$$\mathbf{C} = \begin{pmatrix} C_1 + C_{12} & -C_{12} \\ -C_{12} & C_2 + C_{12} \end{pmatrix}. \tag{5}$$

The diagonal entries correspond to the partial capacitances relative to ground of each island, i.e., the sum of the cross and auto capacitances, while the off-diagonal terms are minus the cross capacitance between the two islands. The diagonal elements are positive, while the off-diagonal ones are negative [66,67]. From the inverse of the capacitance matrix, assuming $C_1 = C_2 = C$, we derive

$$E_C = \frac{e^2}{2}\frac{C + C_{12}}{C^2 + 2CC_{12}} \tag{6}$$

for the islands capacitance and

$$E_{CC} = \frac{e^2}{2}\frac{C_{12}}{C^2 + 2CC_{12}} \tag{7}$$

for the cross-capacitance coupling. It follows that $E_C > E_{CC} > 0$. In the following, we further assume that the parameters of the two mesoscopic islands have been chosen so that they lie within the "charging" regime, in which $E_C/E_J \gg 1$. In this case, Coulomb blockade prevents Cooper pairs from tunneling across the island, except if the back-gate potential is tuned at the degeneracy point between states with different total charge at the island. In our specific case, the single-fermion state associated to the pair of real Majorana modes can be combined into Dirac complex fermion operators, $a_1 = \frac{1}{2}(\gamma_1 + i\gamma_2)$ and $a_2 = \frac{1}{2}(\gamma_3 + i\gamma_4)$, thus allowing for low-energy charge tunneling processes across the impurity involving a single quasiparticle, rather than a Cooper pair. Therefore, setting Q_i at each island so that $Q_i = 2\bar{N}_i + \frac{1}{2}$, with integer $\bar{N}_i$, allows for defining the low-energy subspace at the double junction as spanned by the four states with $\bar{N}_i$ Cooper pairs at island i, with the mode corresponding to a_i full, or empty. Listing those states, together with the corresponding energy eigenvalues, we obtain the set

$$\begin{aligned} &|\bar{N}_1, \bar{N}_2, 0, 0\rangle, \quad \epsilon_{0,0} = \tfrac{1}{2}E_C + \tfrac{1}{4}E_{CC}, \\ &|\bar{N}_1, \bar{N}_2, 1, 1\rangle, \quad \epsilon_{1,1} = \tfrac{1}{2}E_C + \tfrac{1}{4}E_{CC}, \\ &|\bar{N}_1, \bar{N}_2, 1, 0\rangle, \quad \epsilon_{1,0} = \tfrac{1}{2}E_C - \tfrac{1}{4}E_{CC}, \\ &|\bar{N}_1, \bar{N}_2, 0, 1\rangle, \quad \epsilon_{0,1} = \tfrac{1}{2}E_C - \tfrac{1}{4}E_{CC}, \end{aligned} \tag{8}$$

with $|\bar{N}_1, \bar{N}_2, \nu_1, \nu_2\rangle$ denoting the state with $\bar{N}_i$ Cooper pairs at island i and ν_i additional quasiparticle in the level determined by the Majorana modes (clearly, $\nu_i = 0, 1$), and with the energies measured with respect to a common reference level. As we discuss in the following, the level structure summarized in Eqs. (8) is enough to induce an effective Kondo Hamiltonian, except that, in order to recover both SK and CK effects, one has to have a window of values of parameters corresponding to an attractive interisland interaction (that is, E_{CC} has to become <0). This is the main motivation for introducing S, which is coupled to the two islands by a small Josephson term that allows to form a Cooper pair in the superconductor through the annihilation of the two Dirac fermions in the islands, and vice versa. At low energies, only particles populating the a_i levels are involved. Therefore, the corresponding processes are described by the hopping Hamiltonian

$$H_S = -\tau(a_1 a_2 e^{2i\varphi} + a_2^\dagger a_1^\dagger e^{-2i\varphi}). \tag{9}$$

Differently from islands 1 and 2, S hosts no Majorana modes. Therefore, at low energies, charges can enter and exit it only as Cooper pairs. To fix the number of Cooper pairs at S, we assume that it has a finite capacitive energy E_S, which enters the corresponding Hamiltonian given by

$$H_S^{(0)} = -E_{J,S}\cos\chi_S + E_{Q,S}[2N_S - Q_S]^2. \tag{10}$$

As there is no cross-capacitance terms between the two islands and S, the capacitive energy of S is simply given by the inverse of its capacitance, that is $E_S = e^2/(2C_S)$. Tuning $Q_S = 2\bar{N}_S$ and assuming $E_{Q,S}/E_{J,S} > 1$, Coulomb blockade pins at N_S the number of Cooper pairs at S. In this case, charges can tunnel from the islands to S, and vice versa, only in virtual processes. This implies a corresponding lowering of the energy of the states with $\nu_1 = \nu_2 = 0$ and $\nu_1 = \nu_2 = 1$ by an amount that appears at second order in τ and is given by $\epsilon_\tau = -\frac{C_S\tau^2}{4e^2}$. Taking this result and the level diagram in Eqs. (8) altogether, the double-island dynamics is described by the effective Hamiltonian

$$\begin{aligned} H_{\text{Island}}^{\text{Eff}} = \delta(&|0,0\rangle\langle 0,0| + |1,1\rangle\langle 1,1| \\ &- |1,0\rangle\langle 1,0| - |0,1\rangle\langle 0,1|). \end{aligned} \tag{11}$$

To simplify the notation, in Eq. (11) we have omitted the labels associated to the number of Cooper pairs on the two islands. The right-hand side of Eq. (11) depends only on the tuning parameter $\delta = \frac{E_{CC}}{4} - \epsilon_\tau$, which we will use as a control parameter to switch from SK to CK effect. For the following discussion, it is useful to rewrite $H_{\text{Island}}^{\text{Eff}}$ in terms of the Dirac complex fermion operators a_1, a_2 and of their Hermitian conjugates as

$$H_{\text{Island}}^{\text{Eff}} = \delta\{1 - 2[a_1^\dagger a_1 + a_2^\dagger a_2] + 4a_1^\dagger a_1 a_2^\dagger a_2\}. \tag{12}$$

Formally, the coupling between the DSI and the leads is described by the tunneling Hamiltonian H_t, which we model in analogy to what is done in Ref. [59], as

$$H_t = -t\sum_{a=1,2}(c_{0,a}^\dagger a_a + c_{0,a}^\dagger a_a^\dagger e^{-i\omega_a}) + \text{H.c.} \tag{13}$$

In Eq. (13), the term $c_{0,a}^\dagger a_j$ describes the transfer of a fermion from the ith island to the central site of the corresponding lead, with the corresponding depletion of the level

a_j. The term $c^\dagger_{0,a} a^\dagger_a e^{-i\omega_a}$ represents an alternative process through which a fermion is created in the level a_j and another one is created in the corresponding lead along with the annihilation of a Cooper pair in the island by the operator $e^{-i\omega_a}$. Noticeably, this process induces a transition to a state with a higher number of Cooper pairs in the islands, which we rule out on projecting onto the low-energy ground-state manifold of the islands. Therefore, we drop it henceforth from the tunneling Hamiltonian and describe the DSI coupled to the ladder by means of the boundary Hamiltonian $\hat{H}_B$ given by

$$\hat{H}_B = H^{\rm Eff}_{\rm Island} - t \sum_{a=1,2} \{c^\dagger_{0,a} a_a + a^\dagger_a c_{0,a}\}. \tag{14}$$

In addition to the direct tunneling between the leads and the DSI, a local density-density interaction Hamiltonian may arise, as well. The corresponding Hamiltonian $H_{\rm DI}$ can be simply modeled as

$$H_{\rm DI} = \sum_{a,b=1,2} \mu_{a,b} c^\dagger_{0,a} c_{0,a} a^\dagger_b a_b. \tag{15}$$

In the following, we use the boundary Hamiltonian $H_B = \hat{H}_B + H_{\rm DI}$ to discuss the crossover between the SK and the CK regimes at the impurity by also pointing out the remarkable emergence of an intermediate "disconnected lead" (DL) phase, with peculiar properties.

III. EFFECTIVE IMPURITY HAMILTONIAN IN THE VARIOUS REGIMES

To describe the impurity dynamics in our system, we resort to pertinent approximations for $\hat{H}_B$ in different windows of values of the various parameters. In fact, we see that δ is the only scale related to the isolated impurity. The other relevant scales are the tunneling strength t and the local density-density interaction strengths, the $\mu_{a,b}$'s in Eq. (15) which, consistently with our symmetry assumption, we choose so that $\mu_{1,1} = \mu_{2,2} = \mu_{\rm d}$ and $\mu_{1,2} = \mu_{2,1} = \mu_{\rm od}$. A first important limit corresponds to $|\delta| \to \infty$. In this limit, the low-energy manifold of the system is twofold degenerate. In particular, for $\delta \to +\infty$, the two degenerate ground states correspond to the "minidomain walls" of Ref. [68], that is, to the $|1,0\rangle$ and to the $|0,1\rangle$ eigenstates of the DSI, while, for $\delta \to -\infty$, the two degenerate states correspond to the $|0,0\rangle$ and to the $|1,1\rangle$ eigenstates of the DSI.

Leaving aside, for the time being, the density-density interaction encoded in $H_{\rm DI}$ in Eq. (15), we see that, at finite values of the t_a's, tunneling processes between the degenerate ground states are accounted for by resorting to an effective, Kondo-type description of the interaction of the DSI with the leads. To do so, we employ the Schrieffer-Wolff (SW) procedure, which we illustrate in detail in Appendix B. In the symmetric case $t_1 = t_2 = t$, the leading boundary operator describing the residual dynamics within the low-energy subspace of the states of the DSI is either a SK Hamiltonian $H_{\rm K,S}$, in the case $\delta > 0$, or a CK Hamiltonian, $H_{\rm H,C}$, for $\delta < 0$. In particular, on applying the SW transformation to $\hat{H}_B$, one obtains the following:

(i) For $\delta > 0$, the spin Kondo (SK) Hamiltonian $H_{\rm K,S}$ is given by

$$H_{\rm K,S} = J_S \, \vec{S}_0 \cdot \vec{\mathcal{S}} \tag{16}$$

with $J_S = 2t^2/\delta$ and the impurity spin operator $\vec{\mathcal{S}}$ and the lead spin density operator $\vec{S}_j$ defined as

$$\mathcal{S}^\alpha = \frac{1}{2} \sum_{u,u'=1,2} a^\dagger_u \tau^\alpha_{u,u'} a_{u'}, \quad S^\alpha_j = \frac{1}{2} \sum_{u,u'=1,2} c^\dagger_{j,u} \tau^\alpha_{u,u'} c_{j,u'}, \tag{17}$$

with τ^α, $\alpha = x, y, z$ being the Pauli matrices.

(ii) For $\delta < 0$, the charge Kondo (CK) Hamiltonian $H_{\rm K,C}$ is given by

$$H_{\rm K,C} = J_C \, \vec{T}_0 \cdot \vec{\mathcal{T}}, \tag{18}$$

with $J_C = 2t^2/|\delta|$ and the impurity charge-isospin operator $\vec{\mathcal{T}}$ and the lead charge-isospin density operator $\vec{T}_j$ respectively defined as

$$\mathcal{T}^\alpha = \frac{1}{2} \sum_{u,u'=1,2} \tilde{a}^\dagger_u \tau^\alpha_{u,u'} \tilde{a}_{u'}, \quad T^\alpha_j = \frac{1}{2} \sum_{u,u'=1,2} \tilde{c}^\dagger_{j,u} \tau^\alpha_{u,u'} \tilde{c}_{j,u'}, \tag{19}$$

with $\tilde{a}_1 = a_1$, $\tilde{a}_2 = a^\dagger_2$, and $\tilde{c}_{j,1} = c_{j,1}$, $\tilde{c}_{j,2} = c^\dagger_{j,2}$.

Turning on $H_{\rm DI}$ we see that, in the SK regime, it modifies the effective impurity Hamiltonian as

$$H_{\rm K,S} \to \hat{H}_{\rm K,S} = J_S \, \vec{S}_0 \cdot \vec{\mathcal{S}} + \left(\frac{\mu_{\rm d} - \mu_{\rm od}}{2}\right) S^z_0 \mathcal{S}^z + \left(\frac{\mu_{\rm d} + \mu_{\rm od}}{2}\right) \sum_{a=1,2} c^\dagger_{0,a} c_{0,a}, \tag{20}$$

that is, the effective isotropic Kondo Hamiltonian acquires a nonzero anisotropy along the z direction as soon as $\mu_{\rm d} \neq \mu_{\rm od}$ plus a local scattering potential term, which does not substantially affect Kondo physics [2]. At variance, in the complementary CK regime, on turning on $H_{\rm DI}$, we obtain

$$H_{\rm K,C} \to \hat{H}_{\rm K,C} = J_C \, \vec{T}_0 \cdot \vec{\mathcal{T}} + \left(\frac{\mu_{\rm d} + \mu_{\rm od}}{2}\right) \{T^z_0 \mathcal{T}^z + T^z_0 + \mathcal{T}^z\}, \tag{21}$$

that is, again a nonzero anisotropy along the z direction in the (charge) Kondo interaction terms, plus effective, local field contributions coupled to both the impurity- and the itinerant-fermion effective charge-isospin operator at $j = 0$. All the terms appearing at the right-hand side of both Eqs. (20) and (21) are "standard" contributions arising in the Kondo problem and, accordingly, their effect, at least in the simplest case of a perfectly screened spin-$\frac{1}{2}$ impurity, is basically well understood [2].

It is also interesting to address in detail what happens at small values of $|\delta|$. At $\delta = 0$, the leads are fully decoupled from the impurity. At $\delta \neq 0$, to account for the competition between the effects of a finite δ and the hybridization between the a_a modes and the leads [69], we resort to an "all-inclusive" RG analysis, considering the RG equations for all the running couplings associated to $\hat{H}_B$. To do so, we define the dimensionless couplings as $\bar{\tau} = (\frac{D_0}{D})^{1-d_f} (\frac{at}{v})$, $\bar{\mu}_{\rm d,od} = (\frac{a\mu_{\rm d,od}}{v})$, $\bar{\delta} = (\frac{D_0}{D})(\frac{a\delta}{v})$, with $d_f = \frac{1}{2}$. On employing a pertinently adapted

version of the approach used in Refs. [17,19,70], we eventually get the full set of RG equations, given by (apart for irrelevant boundary terms, which can in principle be generated along the RG procedure, and which we neglect in the following)

$$\begin{aligned}
\frac{d\bar{\tau}(D)}{d\,\ln\left(\frac{D_0}{D}\right)} &= (1-d_f)\bar{\tau}(D) + \bar{\mu}_{\rm d}(D)\bar{\tau}(D),\\
\frac{d\bar{\mu}_{\rm d}(D)}{d\,\ln\left(\frac{D_0}{D}\right)} &= -\bar{\delta}(D)\bar{\mu}_{\rm od}(D),\\
\frac{d\bar{\mu}_{\rm od}(D)}{d\,\ln\left(\frac{D_0}{D}\right)} &= -\bar{\delta}(D)\bar{\mu}_{\rm d}(D),\\
\frac{d\bar{\delta}(D)}{d\,\ln\left(\frac{D_0}{D}\right)} &= \bar{\delta}(D) - \frac{\bar{\mu}_{\rm d}(D)\bar{\mu}_{\rm od}(D)}{4}.
\end{aligned} \tag{22}$$

To infer from Eqs. (22) the condition for the crossover between the DL and either the SK or the CK phase, we simplify the right-hand side of Eqs. (22) by neglecting nonlinear terms in the various coupling strengths. Accordingly, the only actually running couplings are now $\bar{\tau}(D)$ and $\bar{\delta}(D)$, given by

$$\bar{\tau}(D) = \left(\frac{D_0}{D}\right)^{1-d_f}\left(\frac{at}{v}\right), \quad \bar{\delta}(D) = \left(\frac{D_0}{D}\right)\left(\frac{a\delta}{v}\right). \tag{23}$$

The derivation of Eqs. (22) relies on the small-coupling assumption for the various boundary interaction strengths. This corresponds to requiring that $\bar{\tau}(D) < 1$, a condition that, if one considers the running coupling strength in Eq. (23), only holds up to $D \sim D_*$, with $D_* \sim D_0\,|\frac{at}{v}|^{\frac{1}{1-d_f}}$. In order for the SW transformation leading to the effective Kondo Hamiltonian to apply, the condition $|t/\delta| < 1$ must hold. From Eqs. (23), one sees that this happens at any scale if $|\delta| > t$ (at the reference scale $D = D_0$). However, due to the nontrivial renormalization of the running parameters, the condition can also be satisfied if $|\delta| < t$. To recover this condition, we note that $\bar{\delta}(D)$ takes over $\bar{\tau}(D)$ at a scale $D_{\rm Cross}$, determined by

$$\bar{\delta}(D_{\rm Cross}) = \bar{\tau}(D_{\rm Cross}) \Rightarrow D_{\rm Cross} = D_0\left(\frac{\delta}{t}\right)^{\frac{1}{d_f}}. \tag{24}$$

Therefore, in order for the Kondo regime to set in, one has to have that $D_{\rm Cross} > D_*$, which implies the condition

$$\frac{a|\delta|}{v} > \left(\frac{at}{v}\right)^{\frac{1}{1-d_f}}. \tag{25}$$

Once the condition in Eq. (25) is satisfied, the impurity dynamics is either described by $\hat{H}_{\rm K,S}$ in Eq. (20), or by $\hat{H}_{\rm K,C}$ in Eq. (21), depending on whether $\delta > 0$ or $\delta < 0$.

At variance, in the DL region the boundary dynamics is described, as we discuss in detail in Appendix C, by the effective local density-density interaction Hamiltonian given by

$$H_{\rm DL} = \kappa c^\dagger_{0,1}c_{0,1}c^\dagger_{0,2}c_{0,2} + \sum_{a=1,2}\lambda_a c^\dagger_{0,a}c_{0,a}, \tag{26}$$

with κ being the effective local interlead density-density interaction strength and λ_1, λ_2 being "residual" intrawire single-body potential scattering strengths.

In the following, we use the results we derived in this section to recover, after resorting to an appropriate low-energy, long-wavelength continuum limit for the fermionic fields in the leads, a detailed RG analysis of the system boundary dynamics in the three phases discussed above.

IV. RENORMALIZATION GROUP ANALYSIS OF THE IMPURITY DYNAMICS

We now resort to a perturbative RG analysis to recover the fixed point (that is, the phase) to which the system flows in the various regions we discuss in the previous section. To do so, we expand the lattice fermionic fields $c_{j,a}$ by retaining only low-energy, long-wavelength excitations around the Fermi points $\pm k_F = \pm\arccos(-\frac{\mu}{2J})$. Therefore, we obtain

$$c_{j,a} \approx \sqrt{a}\,\{e^{ik_F j}\psi_{R,a}(x_j) + e^{-ik_F j}\psi_{L,a}(x_j)\}, \tag{27}$$

with a being the lattice step (which we set to 1 henceforth, except when explicitly required for the sake of the presentation clarity), $x_j = aj$, and $\psi_{R,a}(x)$, $\psi_{L,a}(x)$ being chiral fields described by the $(1+1)$-dimensional Hamiltonian H_0, given by

$$\begin{aligned}
H_0 = -iv\sum_{a=1,2}\int_{-\ell}^{\ell} dx\,\{&\psi^\dagger_{R,a}(x)\partial_x\psi_{R,a}(x)\\
&- \psi^\dagger_{L,a}(x)\partial_x\psi_{L,a}(x)\}.
\end{aligned} \tag{28}$$

To simplify the following derivation we note that, since we are representing the DIS as a pointlike impurity localized at $x = 0$, it is useful to resort to the "even" and "odd" linear combinations of the chiral fermionic fields $\psi_{e,a}(x)$, $\psi_{o,a}(x)$, respectively given by

$$\begin{aligned}
\psi_{e,a}(x) &= \frac{1}{\sqrt{2}}\{\psi_{R,a}(x) + \psi_{L,a}(-x)\},\\
\psi_{o,a}(x) &= \frac{1}{\sqrt{2}}\{\psi_{R,a}(x) - \psi_{L,a}(-x)\}.
\end{aligned} \tag{29}$$

Apparently, $\psi_{o,1}(x)$ and $\psi_{o,2}(x)$ fully decouple from the impurity dynamics, which is accordingly described, in the three different regions identified in Sec. III, by the boundary Hamiltonians

$$\begin{aligned}
\tilde{H}_{\rm K,S} &= 2J_S\,\vec{\sigma}_e(0)\cdot\mathcal{S} + 2\left(\frac{\mu_{\rm d}-\mu_{\rm od}}{2}\right)\sigma^z_e(0)\mathcal{S}^z\\
&\quad + 2\left(\frac{\mu_{\rm d}+\mu_{\rm od}}{2}\right)\rho_e(0),\\
\tilde{H}_{\rm K,C} &= 2J_C\,\vec{\tau}_e(0)\cdot\mathcal{T} + \left(\frac{\mu_{\rm d}+\mu_{\rm od}}{2}\right)\\
&\quad \times\left\{2\tau^z_e(0)\mathcal{T}^z + 2\tau^z_e(0) + \mathcal{T}^z\right\},\\
H_{\rm DL} &= \sum_{a=1,2} 2\lambda_a\rho_{e,a}(0) + 4\kappa\,\rho_{1,e}(0)\rho_{2,e}(0),
\end{aligned} \tag{30}$$

with

$$\begin{aligned}
\rho_{e,a}(0) &= \psi^\dagger_{e,a}(0)\psi_{e,a}(0),\\
\rho_e(0) &= \sum_{a=1,2}\rho_{e,a}(0),\\
\sigma^\alpha_e(0) &= \frac{1}{2}\sum_{u,u'=1,2}\psi^\dagger_{e,u}(0)\tau^\alpha_{u,u'}\psi_{e,u'}(0),\\
\tau^\alpha_e(0) &= \frac{1}{2}\sum_{u,u'=1,2}\tilde{\psi}^\dagger_{e,u}(0)\tau^\alpha_{u,u'}\tilde{\psi}_{e,u'}(0),
\end{aligned} \tag{31}$$

and $\tilde{\psi}_{e,1}(x) = \psi_{e,1}(x)$, $\tilde{\psi}_{e,2}(x) = \psi^{\dagger}_{e,2}(x)$. [Note that the fields $\psi_{e,a}(x)$ contain the combinations of opposite chirality modes that, in each lead, effectively couple to the DIS and can be more general than the symmetric expressions in Eqs. (29). Yet, for the sake of simplicity and without loss of generality in the derivation, in the following we employ the expressions in Eqs. (29), which correspond to symmetric coupling to the DSI of opposite chirality modes in each lead.]

In performing the RG analysis, we neglect the nonpurely Kondo-type terms at the right-hand side of the first two ones of Eqs. (30). This makes us deal with a generally anisotropic Kondo Hamiltonian, using which, in the following, we perform the RG analysis along the guidelines of Ref. [71]. To do so, we note that, in view of the fact that only the $\psi_{e,a}$ fields do actually couple to the impurity spin, the fields in the o sector obey the continuity condition at $x = 0$ given by

$$\psi_{o,a}(0^+) = \psi_{o,a}(0^-) \tag{32}$$

for any value of the Kondo coupling. At zero Kondo coupling, the fields in the e sector satisfy the same boundary conditions as in Eq. (32), that is,

$$\psi_{e,a}(0^+) = \psi_{e,a}(0^-). \tag{33}$$

In general, we expect $\mu_{\rm d} \geqslant \mu_{\rm od}$. Therefore, the RG flow of the dimensionless running coupling strengths in the anisotropic (spin and charge) Kondo Hamiltonians at the right-hand side of Eqs. (30) is described by Eqs. (D5) of Appendix D, switching to the isotropic RG flow of Eq. (D3) in the isotropic limit. In either case, the system flows toward the Kondo fixed point, which accordingly determines a change in the boundary conditions in Eq. (33). In particular, at the SK fixed point one obtains [71]

$$\psi_{e,a}(0^+) = e^{-2i\delta_S}\psi_{e,a}(0^-), \tag{34}$$

with δ_S being a nonuniversal phase shift, which, at the strongly coupled fixed point, is independent of the momentum k measured with respect to the Fermi momentum of the chiral fermion excitations, and is equal to $\frac{\pi}{2}$ if particle-hole symmetry is unbroken [71]. Equation (34) simply corresponds to Nozierès Fermi-liquid boundary conditions, that is, to the fact that the formation of the local Kondo singlet at the impurity location prevents any other electron from accessing that point [3]. From that, taking also into account a possible breaking of the spin rotational symmetry, one obtains that the leading boundary operator allowed at the Kondo fixed point can be expressed as [71]

$$\begin{aligned}\tilde{H}_{\rm K,S} = {} & \alpha_S \psi^{\dagger}_{e,1}(0)\psi_{e,1}(0)\,\psi^{\dagger}_{e,2}(0)\psi_{e,2}(0) \\ & + \sum_{a=1,2} \beta_{S,a}\,\psi^{\dagger}_{e,a}(0)\psi_{e,a}(0)\end{aligned} \tag{35}$$

(see also Appendix B for a systematic derivation of the $\tilde{H}_{\rm K,S}$), with $\psi_{e,a}(0) \equiv \psi_{e,a}(0^-)$ and α_S, $\beta_{S,a}$ appropriate boundary coupling strengths. A similar construction holds for the CK effect, as well, provided one substitutes $\psi_{e,1}(x)$, $\psi_{e,2}(x)$ with $\tilde{\psi}_{e,1}(x)$, $\tilde{\psi}_{e,2}(x)$ defined right after Eqs. (31). As a result, one finds that the noninteracting fixed point is described by the boundary conditions at $x = 0$ given by

$$\tilde{\psi}_{e,a}(0^+) = \tilde{\psi}_{e,a}(0^-), \quad \tilde{\psi}_{o,a}(0^+) = \tilde{\psi}_{o,a}(0^-), \tag{36}$$

and that, at variance, the CK fixed point is described by the boundary conditions

$$\tilde{\psi}_{e,a}(0^+) = e^{-2i\delta_C}\tilde{\psi}_{e,a}(0^-), \quad \tilde{\psi}_{o,a}(0^+) = \tilde{\psi}_{o,a}(0^-). \tag{37}$$

Finally, one also infers that the leading boundary perturbation at the CK fixed point is given by

$$\begin{aligned}\tilde{H}_{\rm K,C} = {} & \alpha_C \tilde{\psi}^{\dagger}_{e,1}(0)\tilde{\psi}_{e,1}(0)\,\tilde{\psi}^{\dagger}_{e,2}(0)\tilde{\psi}_{e,2}(0) \\ & + \sum_{a=1,2} \beta_{C,a}\,\tilde{\psi}^{\dagger}_{e,a}(0)\tilde{\psi}_{e,a}(0),\end{aligned} \tag{38}$$

with $\tilde{\psi}_{e,a}(0) \equiv \tilde{\psi}_{e,a}(0^-)$ and α_C, $\beta_{C,a}$ interaction strengths. Remarkably, the leading boundary Hamiltonian at both the SK and CK fixed point reported in Eqs. (35) and (38), takes exactly the same form as the leading boundary Hamiltonian in the DL region, the third one of Eqs. (30). As we discuss in the following, this allows for simplifying the derivation by making an unified analysis of the ac conduction properties of the system at each one of the three fixed points.

Before concluding this section, we now briefly mention the effects of the local magnetic field acting on both the impurity spin and the spin of the conduction electrons in the effective Kondo Hamiltonians on the first two lines of Eqs. (30). In fact, while, in general, a strong applied field may eventually lead to the suppression of Kondo effect, it is by now well established that the Kondo effect instead survives the applied field, as long as T_K is higher than the energy scale associated to the applied magnetic field [17,72]. The local magnetic field encodes the local density-density interaction at the DSI. This is a minor effect, which is expected to be much smaller than the direct electronic tunneling encoded in $\hat{H}_B$ in Eq. (14). This implies that T_K is expected to be always much larger than the energy scale associated to the Zeeman term, which does not spoil the Kondo effect. Based on these observations, we now discuss the leading boundary perturbation at both the Kondo and the DL fixed points. As we discuss above, basically $H_{\rm DL}$ in Eqs. (30) encompasses both the boundary Hamiltonians in Eqs. (35) and (38). Therefore, we refer to $H_{\rm DL}$ for our further analysis. As noted in Appendix D, a simple power counting implies that the dimensionless coupling associated to κ is $\mathcal{K}(D) = \frac{D}{D_0}\kappa$. On lowering the running cutoff D, one therefore obtains that $\mathcal{K}(D)$ scales to 0 as D/D_0. Thus, we conclude that the interwire local density interaction is an irrelevant perturbation at either the SK (CK), or at the DL fixed point, which is consistent with the expected stability of the various fixed points. The leftover terms are, instead, marginal one-body scattering potential terms. These marginally deform the fixed-point dynamics by changing the phase shift in the e channel, with minor consequences on the ac conduction properties of the system, as we discuss in the following.

V. AC CONDUCTANCE AND PHASE DIAGRAM OF THE SYSTEM

In this section, referring to the results we derive in detail in Appendix E, we evidence how it is possible to map out the whole phase diagram of our tunable Kondo device by means of the ac conductance tensor and of its dependence on the frequency ω. To perform our analysis, in the following we mostly focus onto the ac conduction properties of the system *across* the impurity, both over the same lead, and on different leads. Specifically, consistently with the symmetries of our system, we discuss [in the notation of Eq. (A7) of Appendix A], the intralead ac conductance, $\mathbf{G}_{(1,>);(1,<)}(\omega)$, and the interlead one, $\mathbf{G}_{(2,>);(1,<)}(\omega)$, as a function of ω. As we extensively discuss in the following, whether $\mathbf{G}_{(2,>);(1,<)}(\omega)$ is zero or not and, in this latter case, whether it takes the same sign as $\mathbf{G}_{(1,>);(1,<)}(\omega)$, or the two of them have opposite signs, allows us to discriminate between the various phases of our system. To provide a comprehensive sample of the behavior of the ac conductance tensor as a function of ω, in the following we discuss in detail both the relevant regimes $\omega \gg kT_K \gg kT$ (perturbative regime) and $kT \ll \omega \ll kT_K$ (Kondo fixed-point regime).

We now discuss in detail the various regions.

A. AC conductance in the spin Kondo phases

Within the SK phase, the impurity dynamics is described by $\hat{H}_{\mathrm{K,S}}$ in Eq. (20). As it is not relevant for the purpose of our discussion, we leave aside the one-body scattering term henceforth and perform the following derivation by using the anisotropic Kondo Hamiltonian $H^{\mathrm{anis}}_{\mathrm{K,S}}$, given by

$$H^{\mathrm{anis}}_{\mathrm{K,S}} = J_{S,\perp}\,\{\mathcal{S}^{+}\sigma^{-}(0) + \mathcal{S}^{-}\sigma^{+}(0)\} + J_{S,z}\,\mathcal{S}^{z}\sigma^{z}(0). \quad (39)$$

Consistently with the microscopic derivation of $H^{\mathrm{anis}}_{\mathrm{K,S}}$, we expect that both $J_{S,\perp}$ and $J_{S,z}$ are >0. Moreover, since μ_{d} and μ_{od} are both >0 and one "naturally" expects $\mu_{\mathrm{d}} \geqslant \mu_{\mathrm{od}}$, the RG trajectories induced by $H^{\mathrm{anis}}_{\mathrm{K,S}}$ all lie within region I of the diagram in Fig. 6 of Appendix D. According to Eqs. (D5) and (D6), at a given value of the RG invariant $H = -\mathcal{J}^2_{S,z} + \mathcal{J}^2_{S,\perp}$, with $\mathcal{J}_{S,\perp(z)} = \frac{aJ_{S,\perp(z)}}{v}$ (note that, according to the above discussion, one typically gets $H < 0$), the RG flow induced by the spin Kondo Hamiltonian is encoded in the running dimensionless coupling $\mathcal{J}_{S,\perp}(D)$, with the running scale D to be identified with ω (which, as stated above, we assume to be $\gg kT$). By integrating the second-order RG equations for the running coupling strength [Eqs. (D5)], one obtains (trading the dependence on D for an explicit dependence on ω)

$$\mathcal{J}_{S,\perp}(D=\omega) = \frac{2\sqrt{|H|}\left(\frac{kT_K}{\omega}\right)^{\sqrt{|H|}}}{1-\left(\frac{kT_K}{\omega}\right)^{2\sqrt{|H|}}}, \quad (40)$$

with the Kondo temperature $kT_K = D_0\{\frac{\mathcal{J}_z(D_0)-\sqrt{|H|}}{\mathcal{J}_z(D_0)+\sqrt{|H|}}\}^{\frac{1}{2\sqrt{|H|}}}$, D_0 being the reference energy scale (high-energy cutoff) and $\mathcal{J}_z(D_0) = \frac{aJ_{S,\parallel}}{v}$ (note that, in our specific case, since, in order for the SW transformation leading to $H_{\mathrm{K,S}}$ and to $H_{\mathrm{K,C}}$ to apply, we have to assume that there are no physical processes involving energies of the order of $|2\delta|$, we must properly set $D_0 = |2\delta|$).

In Appendix D we also show how, in the isotropic limit $H = 0$, one obtains

$$\mathcal{J}_{S,\perp}(D=\omega) = \mathcal{J}_{S,z}(D=\omega) = \frac{1}{\ln\left(\frac{kT_K}{\omega}\right)}, \quad (41)$$

with now T_K given by

$$kT_K = D_0 e^{-\frac{1}{\mathcal{J}_\perp(D_0)}}. \quad (42)$$

So, from Eqs. (40) and (41), we eventually conclude that, both in the anisotropic and in the isotropic cases, the running coupling strength is a scaling function of the dimensionless ratio $\omega/(kT_K)$.

In order to incorporate the nontrivial RG flow in Eqs. (40) and (41) into the formulas for the ac conductances, we refer to the derivation of Appendix E 1. Specifically, keeping $\omega > kT, kT_K$ and using it as the running energy scale, we obtain for the running intralead and interlead ac conductances $\mathbf{G}_{(1,>);(1,<)}(\omega)$ and $\mathbf{G}_{(2,>);(1,<)}(\omega)$ the result in Eq. (E12) of Appendix E 1, that is,

$$\mathbf{G}_{(1,>);(1,<)}(\omega) = -\frac{e^2}{2\pi}\left\{1 - \mathcal{J}^2_{S,\perp}(\omega)\right\},$$
$$\mathbf{G}_{(2,>);(1,<)}(\omega) = -\frac{e^2}{2\pi}\mathcal{J}^2_{S,\perp}(\omega). \quad (43)$$

As stated in Appendix E 1, the result in Eq. (43) is expected to apply from $\omega \sim D_0$ all the way down to $\omega \sim kT_K$. From the right-hand side of Eq. (43) we see that turning on the Kondo coupling implies a reduction in the intralead ac current together with a nonzero interlead current. This is due to the peculiar features of the Kondo processes mediating the ac transport at nonzero coupling to the impurity. In terms of electron transmission across the impurity, transport from, say, lead 1 to the same lead does not correspond to a change in the "spin index" of the transmitted electron. At the onset of Kondo dynamics, together with the former scattering process, which we depict in Fig. 3(a) as a particle-to-particle transmission within lead 1, impurity spin-flip processes can induce single-electron tunneling from lead 1 to lead 2, mediated by the coupling to the impurity spin $\vec{\mathcal{S}}$. This process, which we depict in Fig. 3(b) as a particle-to-particle transmission from lead 1 to lead 2, is what is responsible for a nonzero $\mathbf{G}_{(2,>);(1,<)}(\omega)$. This is a relevant process as ω goes down from D_0 to kT_K. Accordingly, we find that the corresponding off-diagonal conductance takes over, when going down with ω, until one enters the Kondo regime at the scale kT_K. An important observation is that, since the current induced in lead 2 is due to particle-to-particle transmission processes, it takes the same sign as the current in lead 1. This is evidenced in Eq. (43) by the fact that, as long as the perturbative RG approach holds (that is, for $\omega > kT_K$), one has that both $\mathbf{G}_{(1,>);(1,<)}(\omega)$ and $\mathbf{G}_{(2,>);(1,<)}(\omega)$ are <0 (with the $-$ sign due to our conventional definition of the positive direction for the current operators as the one pointing toward the impurity both from the left- and right-hand sides of the system).

On flowing toward the SK fixed point, the spin density of the lead electrons at $x = 0$ "locks together" with the impurity spin, so to effectively cut the system into two separate parts. Accordingly, there is 0 interlead ac conductance, that is, $\mathbf{G}_{(2,>);(1,<)}(\omega) = 0$. Moreover, as the (Nozières-type) SK

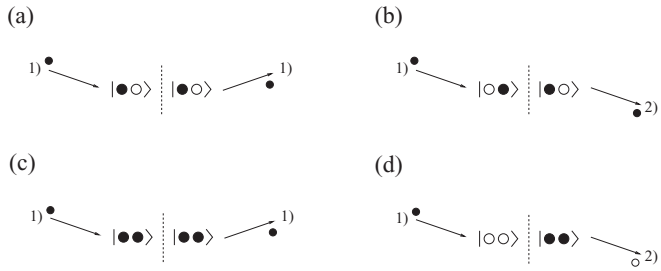

FIG. 3. Sketch of the possible single-particle transmission processes that can take place in either the SK, or the CK, phase, if an incoming particle from lead 1 hits the effective magnetic impurity. The ket represents the "impurity" state, so that a filled (empty) dot corresponds to the full (empty) state corresponding to the fermionic mode a_1 (left-hand dot) or a_2 (right-hand dot) in Eq. (12). (a) In the SK phase, the particle from lead 1 is transmitted as a particle toward the same lead. The impurity state is $|\Uparrow\rangle$ before, and after, the scattering process. (b) Still in the SK phase, the particle from lead 1 is transmitted as a particle toward lead 2. The impurity state is $|\Downarrow\rangle$ before the scattering process and switches to $|\Uparrow\rangle$ after, consistently with total spin conservation. (c) In the CK phase, the particle from lead 1 is transmitted as a particle toward the same lead. The impurity state is $|\Uparrow\rangle$ before, and after, the scattering process. (d) Still in the CK phase, the particle from lead 1 is transmitted as a hole toward lead 2 (crossed Andreev reflection). The impurity state is $|\Downarrow\rangle$ before the scattering process and switches to $|\Uparrow\rangle$ after, consistently with total charge conservation. Remarkably, total charge conservation forbids crossed Andreev reflection with the hole transmitted toward lead 1.

fixed point is described in terms of the single-electron phase shift δ_S, we may employ Eq. (A21) to obtain

$$\mathbf{G}_{(1,>);(1,<)}(\omega) = -\frac{e^2}{2\pi}\cos^2(\delta_S). \tag{44}$$

In the particle-hole-symmetric case (corresponding to a total phase shift $\delta_S = \frac{\pi}{2}$ in the e-linear combinations of the chiral fields in each channel), Eq. (44) implies $\mathbf{G}_{(1,>);(1,<)}(\omega) = 0$. More generally, for $\delta_S \neq \frac{\pi}{2}$, one expects a reduction of $\mathbf{G}_{(1,>);(1,<)}(\omega)$ by a factor $\cos^2(\delta_S)$ and a simultaneous suppression of $\mathbf{G}_{(2,>);(1,<)}(\omega)$.

The leading boundary perturbation at the SK fixed point is the same as the one at the DL fixed point, that is, $\tilde{H}_{\mathrm{K,S}}$ in Eq. (35). In fact, the term at the right-hand side of Eq. (35) that might potentially contribute a nonzero $\mathbf{G}_{(2,>);(1,<)}(\omega)$ is the one $\propto\alpha_S$. Yet, in analogy with the calculations in the DL phase of Appendix E 2, we find that $\mathbf{G}_{(2,>);(1,<)}(\omega) = 0$, at least to second order in α_S [in fact, as long as the boundary interaction describes electron scattering off a local singlet, one is expected to obtain $\mathbf{G}_{(2,>);(1,<)}(\omega) = 0$ at any order in α_S] while, to order α_S^2, we obtain

$$\mathbf{G}_{(1,>);(1,<)}(\omega) = -\frac{e^2}{2\pi}\left\{\cos^2(\delta_S) - \frac{8\pi\,\cos(2\delta_S)\alpha_S^2\omega^2}{3v^2}\right\}. \tag{45}$$

In particular, in the particle-hole-symmetric case, one has $2\delta_S = \pi$, which implies

$$\mathbf{G}_{(1,>);(1,<)}(\omega) = -\frac{e^2}{2\pi}\,\frac{8\pi\alpha_S^2\omega^2}{3v^2}. \tag{46}$$

To summarize, we have shown that, on lowering ω from $\omega \sim D_0$ to $\omega \sim kT_K$, $\mathbf{G}_{(1,>);(1,<)}(\omega)$ is suppressed by the Kondo interaction. At the same time, the relevance of the "effective" spin-flip processes induces a nonzero $\mathbf{G}_{(2,>);(1,<)}(\omega)$, which increases as ω is lowered toward kT_K. Since a spin-flip process here corresponds to a particle/hole tunneling from one lead as an injected particle/hole to the other one, the ac currents induced in the two leads by means of a voltage bias applied to either one of them flow toward the same directions. Once the system has flown to the SK fixed point, it may, or may not, exhibit a finite $\mathbf{G}_{(1,>);(1,<)}(\omega)$, depending on whether particle-hole symmetry is broken, or not [6]. The leading correction to the ac conductance tensor is diagonal, as well, and $\propto\omega^2$, consistently with Nozières Fermi-liquid theory [3].

B. The ac conductance in the charge-Kondo phases

Within the CK phase, the impurity dynamics is described by the Hamiltonian $\hat{H}_{\mathrm{K,C}}$ in Eq. (21). Aside from the CK coupling, $\hat{H}_{\mathrm{K,C}}$ contains a Zeeman-type coupling to a local magnetic field of both $\tau^z(0)$ and $\mathcal{T}^z$. Out of these two terms, the former one provides an additional phase shift to single-electron scattering amplitudes which is different in different leads. Again, this just quantitatively affects the calculation of the ac conductance, without invalidating the whole RG analysis of the Kondo interaction. The effects of the term $\propto\mathcal{T}^z$ are discussed in Appendix D. Here, we just mention that this term is not expected to substantially affect the Kondo physics as long as the energy scale associated to the local magnetic field is much lower than kT_K [17,72,73]. Having stated this, one therefore readily sees that the calculation of the ac conductance in the CK case can be performed in perfect analogy as what we have done in Sec. V A for the SK case. Yet, a fundamental difference in the results for the ac conductance in the CK case compared to the SK effect arises from the different nature of physical processes yielding a nonzero $\mathbf{G}_{(2,>);(1,<)}(\omega)$ in the two cases. Indeed, while, in the CK case, interlead charge tunneling is still supported by an impurity spin flip, this process now corresponds to a switch between local states with a net charge difference equal to $\pm 2e$. Thus, charge is conserved in a single scattering process only modulo 2 and, in particular, interlead scattering processes are of Andreev type, with an incoming particle from lead 1 emerging as an outgoing hole in lead 2. At variance, intralead scattering processes again correspond to particle-to-particle (hole-to-hole) scattering events. In Fig. 3(c) we depict intralead scattering processes in the charge Kondo phase, while in Fig. 3(d) we draw a sketch of a single "crossed-Andreev-reflection"–like scattering event from lead 1 to lead 2, supporting interlead ac transport. As a result, we now expect that $\mathbf{G}_{(1,>);(1,<)}(\omega)$ and $\mathbf{G}_{(2,>);(1,<)}(\omega)$ have opposite sign. Indeed, for $D_0 \gtrsim \omega \gtrsim kT_K$, one obtains

$$\begin{aligned}\mathbf{G}_{(1,>);(1,<)}(\omega) &= -\frac{e^2}{2\pi}\left\{1 - \mathcal{J}_{C,\perp}^2(\omega)\right\},\\ \mathbf{G}_{(2,>);(1,<)}(\omega) &= \frac{e^2}{2\pi}\mathcal{J}_{C,\perp}^2(\omega),\end{aligned} \tag{47}$$

that is, Eqs. (E11) of Appendix E 1, with $\mathcal{J}_{C,\perp}(\omega)$ being a scaling function of $\omega/(kT_K)$ defined just as $\mathcal{J}_{S,\perp}(\omega)$ of Eqs. (40) and (41) by replacing the spin Kondo couplings

with the corresponding charge Kondo ones. As at the SK fixed point, again, when flowing toward the CK fixed point, the charge-isospin density of the lead electrons at $x = 0$ "locks together" with the impurity spin, so to effectively cut the system into two separate parts. Again, if δ_C is the corresponding intralead single-fermion phase shift, this implies a reduction of $\mathbf{G}_{(1,>);(1,<)}(\omega)$ by a factor $\cos^2(\delta_C)$ and a simultaneous suppression of $\mathbf{G}_{(2,>);(1,<)}(\omega)$. The leading boundary operator at the CK fixed point is given by $\tilde{H}_{\mathrm{K,C}}$ in Eq. (38). Just as in the spin Kondo case, we therefore obtain, to order α_C^2, that $\mathbf{G}_{(2,>);(1,<)}(\omega)$ keeps $= 0$, while $\mathbf{G}_{(1,>);(1,<)}(\omega)$ is corrected as

$$\mathbf{G}_{(1,>);(1,<)}(\omega) = -\frac{e^2}{2\pi}\left\{\cos^2(\delta_C) - \frac{8\pi\ \cos(2\delta_C)\alpha_C^2\omega^2}{3v^2}\right\}. \tag{48}$$

To summarize the results of this section, we see that on lowering ω, just as in the SK case, $\mathbf{G}_{(1,>);(1,<)}(\omega)$ is reduced by the Kondo interaction, while the relevance of the "effective" spin-flip processes induces a nonzero $\mathbf{G}_{(2,>);(1,<)}(\omega)$. Since, now, a spin-flip process corresponds to a particle/hole from one lead as injected as a hole/particle into the other one, $\mathbf{G}_{(1,>);(1,<)}(\omega)$ and $\mathbf{G}_{(2,>);(1,<)}(\omega)$ have opposite signs. Finite-ω contributions to $\mathbf{G}_{(1,>);(1,<)}(\omega)$ at the CK fixed point are $\propto\omega^2$, again consistently with Nozières Fermi-liquid theory [3].

C. The ac conductance in the decoupled lead phase

The DL phase is characterized by the irrelevant boundary interaction H_{DL} in Eq. (30). In Appendix E 2 we show how, in the decoupled lead phase, our system is expected to have $\mathbf{G}_{(2,>);(1,<)}(\omega) = 0$ and

$$\mathbf{G}_{(1,>);(1,<)}(\omega) \approx -\frac{e^2}{2\pi}\left\{\cos^2(\delta_\kappa) - \frac{8\ \cos(2\delta_\kappa)\kappa^2\omega^2}{3\pi^2 v^2}\right\}, \tag{49}$$

with δ_κ single-fermion phase shift at the DL fixed point. On top of the result in Eq. (49) it is also worth stressing that, since the boundary interaction describing the impurity throughout the decoupled lead phase is irrelevant, there is no "Kondo-type" expected crossover in this region, on lowering ω. Thus, we may eventually conclude that, lowering ω at fixed system parameters, the Kondo-type phases are dramatically different from the non-Kondo-type one in that first of all the former ones are characterized by a strong dependence on ω of ac conductance tensor, as ω is lowered toward kT_K, while the latter one just exhibits a mild dependence on ω, and is almost not at all affected by the coupling of the leads to the superconducting island. Second, the fixed-point properties are dramatically different, as well. Indeed, when lying within either one of the Kondo phases, $\mathbf{G}_{(1,>);(1,<)}(\omega)$ is strongly reduced by the formation of the Kondo singlet at the DSI and is eventually forced to be $=0$ if particle-hole symmetry is not broken. At variance, at the DL fixed point, $\mathbf{G}_{(1,>);(1,<)}(\omega)$ is in general finite and only limited by possible one-body scattering potential terms due to the coupling to the DSI.

The results of this section allow for fully mapping out the phase diagram of the system by looking at the ac conductance tensor of the device as a function of both ω and of the control parameter δ, as we summarize in the following.

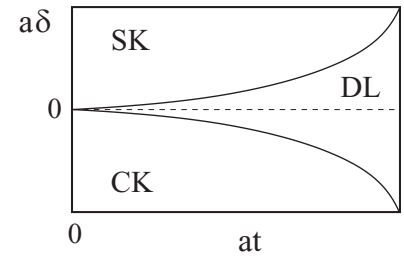

FIG. 4. Boundary phase diagram of our system in the at-$a\delta$ plane: for $|\delta| < v^{\frac{d_f}{d_f-1}}\,(at)^{\frac{1}{1-d_f}}$ the decoupled lead phase sets in. For $\delta > v^{\frac{d_f}{d_f-1}}\,(at)^{\frac{1}{1-d_f}}$ and for $\delta < -v^{\frac{d_f}{d_f-1}}\,(at)^{\frac{1}{1-d_f}}$, the spin Kondo and the charge Kondo phase, respectively, sets in.

D. The ac transport properties and phase diagram of the system

Referring to the phase diagram of Fig. 4, in the following we use as tuning parameter $r = \delta v/(at^2)$. In particular, at $r = \pm 1$, the system undergoes two transitions between either the SK, or the CK, phase (for $|r| > 1$) and the DL phase (for $|r| < 1$). The three different phases can be well characterized by looking at the ac conductances as a function of ω, from $\omega \sim D_0$ all the way down across $\omega \sim kT_K$ and below.

In Fig. 5 we show the expected behavior of $\mathbf{G}_{(1,>);(1,<)}(\omega)$, as well as of $\mathbf{G}_{(2,>);(1,<)}(\omega)$, as a function of ω in the three phases. In the DL phase one sees a very mild dependence of $\mathbf{G}_{(1,>);(1,<)}(\omega)$ on ω, with $\mathbf{G}_{(2,>);(1,<)}(\omega)$ being constantly $=0$. At variance, for $r > 1$ (SK phase), $\mathbf{G}_{(1,>);(1,<)}(\omega)$ drops to 0 on lowering ω, with a crossover scale determined by kT_K. At the same time, $\mathbf{G}_{(2,>);(1,<)}(\omega)$ first rises and then drops to 0, as well, for $\omega < kT_K$. As we discuss above, in Sec. V A, in this phase, $\mathbf{G}_{(1,>);(1,<)}(\omega)$ and $\mathbf{G}_{(2,>);(1,<)}(\omega)$ have the same sign, in the window of values of ω in which both are nonzero. Finally, for $r < -1$ (charge Kondo phase) $\mathbf{G}_{(1,>);(1,<)}(\omega)$ and $\mathbf{G}_{(2,>);(1,<)}(\omega)$ behave as in the spin Kondo phase, but now, in the window of values of ω in which both are nonzero, they have opposite sign.

A complementary, alternative analysis can instead be performed by sweeping r (that is, δ) and by looking at how the interlead ac conductance $\mathbf{G}_{(2,>);(1,<)}(\omega)$ varies at fixed ω ($> kT_K$). As stated in Sec. V C, we expect $\mathbf{G}_{(2,>);(1,<)}(\omega) = 0$ within the DL phase, for $|r| < 1$. Crossing the boundary at $r = \pm 1$ from within the DL phase, one enters either one of the Kondo phases, in which $\mathbf{G}_{(2,>);(1,<)}(\omega) \neq 0$, with a sign depending on whether one is looking at the SK or at the CK phase. Thus, detecting the onset, along the r axis, of regions with $\mathbf{G}_{(2,>);(1,<)}(\omega) \neq 0$, separated by a zero interlead ac conductance, provides another means to probe the phase diagram of our system.

Finally, we note that, denoting with $T_K(\delta)$ the Kondo temperature as a function of δ, once all the other system parameters are fixed since, according to the scaling assumption for the Kondo effect, one expects the conductance to be a scaling function of $\omega/(kT_K(\delta))$ [74,75], increasing $|\delta|$ [that is, increasing $T_K(\delta)$] is in principle equivalent to lowering

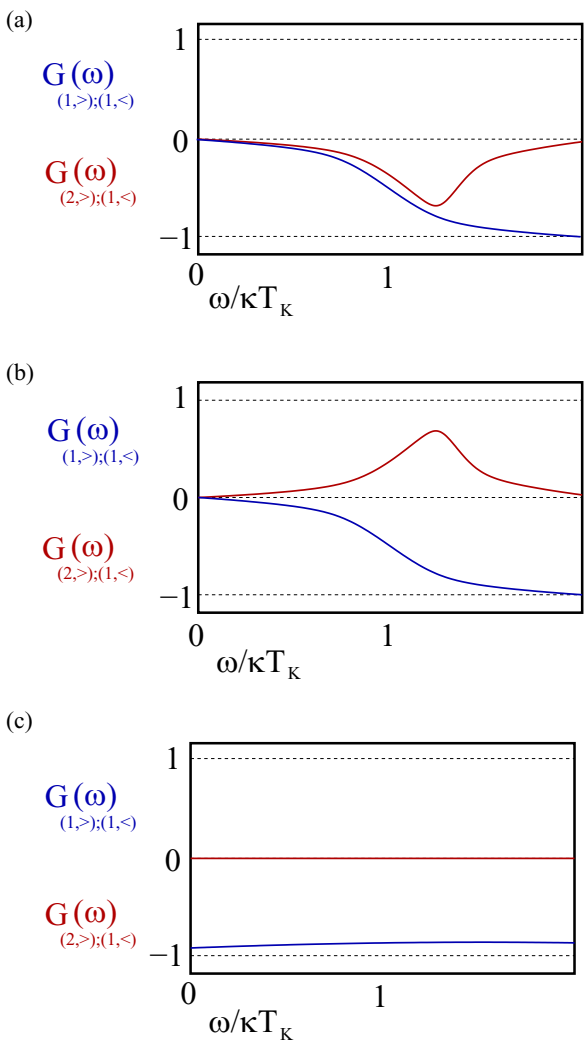

FIG. 5. Sketch of $\mathbf{G}_{(1,>);(1,<)}(\omega)$ and of $\mathbf{G}_{(2,>);(1,<)}(\omega)$ as a function of ω in the various phases of the system, determined by different values of $r = \delta v/(at^2)$ and for $\omega, kT_K \gg kT$. From top to bottom: (a) Expected behavior of $\mathbf{G}_{(1,>);(1,<)}(\omega)$ (blue curve) and $\mathbf{G}_{(2,>);(1,<)}(\omega)$ (red curve) in units of $e^2/(2\pi)$ as a function of ω/kT_K in the SK region ($r > 1$). The saturation of $\mathbf{G}_{(1,>);(1,<)}(\omega)/[e^2/(2\pi)]$ at high values of ω/kT_K may take place to values lower than 1, depending on the presence of potential scattering terms. Breaking of particle-hole symmetry may give rise to a nonzero saturation value of $\mathbf{G}_{(1,>);(1,<)}(\omega)/[e^2/(2\pi)]$ as $\omega \to 0$ (see main text for details). (b) Expected behavior of $\mathbf{G}_{(1,>);(1,<)}(\omega)$ (blue curve) and $\mathbf{G}_{(2,>);(1,<)}(\omega)$ (red curve) in units of $e^2/(2\pi)$ as a function of ω/kT_K in the CK region ($r < -1$). Again, potential scattering terms can make $\mathbf{G}_{(1,>);(1,<)}(\omega)/[e^2/(2\pi)]$ saturate to values lower than 1 at high values of ω/kT_K and breaking of particle-hole symmetry may give rise to a nonzero saturation value of $\mathbf{G}_{(1,>);(1,<)}(\omega)/[e^2/(2\pi)]$ as $\omega \to 0$. (c) Expected behavior of $\mathbf{G}_{(1,>);(1,<)}(\omega)$ (blue curve) and $\mathbf{G}_{(2,>);(1,<)}(\omega)$ (red curve) in units of $e^2/(2\pi)$ as a function of ω/T_K in the DL region ($-1 < r < 1$). Due to the absence of a physically meaningful temperature reference scale in this region, ω has rescaled in units of what would be kT_K for the specified values of the system's parameters in that region if Kondo effect were taking place.

ω toward kT_K. So, one expects plots similar to the ones in Fig. 5 but, now, using δ as a control parameter. This might in principle provide an easier way to probe Kondo scaling in our system since δ can actually be used as a control parameter of the device.

Therefore, we may readily conclude how pertinently changing either ω or δ (or both), one can in principle probe the whole phase diagram of the system and, in particular, the remarkable possibility of switching from SK to CK effect by acting upon one control parameter only.

VI. CONCLUDING REMARKS

In this paper, we propose how to engineer a tunable Kondo system which, depending on the value of in principle one parameter only, can either work as a spin Kondo or as a charge Kondo impurity. Gauging the control parameter δ, one moves the system from the SK to the CK phase, passing across an intermediate, DL phase, in which the Kondo impurity is effectively irrelevant for the ac conduction properties of the system. While the main architecture of our device can appear rather complicated, we are confident that our theoretical proposal can potentially raise the interest in employing the interplay between emerging Majorana modes in condensed matter physics and Kondo effect to experimentally engineer an efficient tunable Kondo device.

Within linear response theory, we derive the intralead and the interlead ac conductance of the system as a function of the frequency ω throughout the whole phase diagram. As a result, we show how the two conductances provide an effective means to identify, and distinguish from each other, the SK, CK, and DL phases of the system. To engineer our system, we employ a minimal setup, with only two spinless fermionic leads. In principle, nowadays technology allows for realizing spinless, one-dimensional electronic conduction channels at, for instance, semiconductor nanowires with a strong Rashba spin-orbit interaction and Zeeman energy [76], as well as edge states of a spin-Hall insulator [77]. So, we expect it to be possible to realize our model, in a realistic experiment, with spinless leads, which would rule out unwanted complications on top of the minimal physics we describe here, such as onset of multichannel either SK or CK phases which, nevertheless, we plan to study in a future work.

Finally, it is also worth recalling how, within the CK phase, our Kondo impurity triggers interwire conduction via a peculiar crossed Andreev reflection between the two leads, which suggests that, in a "dual" setup, in which a Cooper pair is injected into the leads through the DSI, our system might realize an efficient long-distance electronic entangler.

ACKNOWLEDGMENT

A.N. acknowledges financial support by the European Union, under ERC FIRSTORM, Contract No. 692670.

APPENDIX A: EQUILIBRIUM AC CONDUCTANCE TENSOR IN THE CASE OF A QUANTUM POINT CONTACT BETWEEN TWO WIRES

In this Appendix, we briefly review the formula for the equilibrium ac conductance tensor in the case in which there is a simple structureless quantum point contact between two quantum wires, located at $x = 0$, between the two wires. The purpose of extensively studying the simple model addressed in the following is twofold. On one hand, starting from the lattice model Hamiltonian and eventually resorting to the continuum formulation of the system allows us to define the general framework within which we compute the ac conductance tensor throughout our paper. On the other hand, some of the results we obtain along the derivation of this Appendix are important to ground the discussion of the other, more complex, cases discussed in the paper.

As a starting point, we consider the lattice model Hamiltonian given by

$$H_{\mathrm{PC;Lat}} = \sum_{a=1,2} \left\{ -J \sum_{j=-\ell}^{\ell-1} [c^{\dagger}_{j,a} c_{j+1,a} + c^{\dagger}_{j+1,a} c_{j,a}] - \mu \sum_{j=-\ell}^{\ell} c^{\dagger}_{j,a} c_{j,a} \right\} + H_B, \tag{A1}$$

with the impurity Hamiltonian H_B given by

$$H_B = V_d \sum_{a=1,2} c^{\dagger}_{0,a} c_{0,a} + V_{od} \{ c^{\dagger}_{0,1} c_{0,2} + c^{\dagger}_{0,2} c_{0,1} \}. \tag{A2}$$

To define the ac conductance tensor, we imagine our device to be composed of four different regions $(1, <)$, $(1, >)$, $(2, <)$, $(2, >)$, each one containing the sites at either the left- or the right-hand side of the point contact, with the site at $j = 0$ "evenly shared" between the two regions. In practice, we define the charge operator at each region so that

$$Q_{a,<} = e \sum_{j=-\ell}^{-1} c^{\dagger}_{j,a} c_{j,a} + \frac{e}{2} c^{\dagger}_{0,a} c_{0,a}, \quad Q_{a,>} = e \sum_{j=1}^{\ell} c^{\dagger}_{j,a} c_{j,a} + \frac{e}{2} c^{\dagger}_{0,a} c_{0,a}. \tag{A3}$$

Defining the corresponding current operators as $I_{a,\lambda}(t) = \frac{dQ_{a,\lambda}(t)}{dt}$, with $\lambda = <, >$, we consider the average current in region a, λ, $\mathcal{I}_{(a,\lambda)}(t)$, arising when each region a', λ' is biased with a time-dependent voltage $v_{a',\lambda'}(t)$. Within linear response theory, we obtain

$$\begin{aligned} \mathcal{I}_{(a,\lambda)}(t) &= \langle I_{a,\lambda}(t) \rangle = -i \sum_{a',\lambda'} \int_{-\infty}^{t} dt'\, v_{a',\lambda'}(t') \langle [I_{a,\lambda}(t), Q_{a',\lambda'}(t')] \rangle \\ &\equiv \sum_{a',\lambda'} \int_{-\infty}^{\infty} dt\, \mathcal{G}_{(a,\lambda);(a',\lambda')}(t - t') v_{a',\lambda'}(t'), \end{aligned} \tag{A4}$$

with the retarded Green's function

$$\mathcal{G}_{(a,\lambda);(a',\lambda')}(t - t') = -i\theta(t - t') \langle [I_{a,\lambda}(t), Q_{a',\lambda'}(t')] \rangle. \tag{A5}$$

Resorting to Fourier space, one therefore readily obtains the ac conductance tensor. To do so, one starts from the Fourier transform of the function in Eq. (A5), given by

$$\mathcal{G}_{(a,\lambda);(a',\lambda')}(\omega) = \int_{-\infty}^{\infty} dt\, e^{i\omega t}\, \mathcal{G}_{(a,\lambda);(a',\lambda')}(t). \tag{A6}$$

Denoting with $\mathbf{G}_{(a,\lambda);(a',\lambda')}(\omega)$ the corresponding element of the ac conductance tensor, one therefore obtains [78]

$$\mathbf{G}_{(a,\lambda);(a',\lambda')}(\omega) = \tfrac{1}{2} \{ \mathcal{G}_{(a,\lambda);(a',\lambda')}(\omega) + \mathcal{G}_{(a,\lambda);(a',\lambda')}(-\omega) \}. \tag{A7}$$

Finally, on defining the current-current retarded Green's function

$$\mathcal{G}^{I}_{(a,\lambda);(a',\lambda')}(t - t') = -i\theta(t - t') \langle [I_{a,\lambda}(t), I_{a',\lambda'}(t')] \rangle, \tag{A8}$$

one readily sees, by differentiating with respect to t both sides of Eq. (A8) and switching back to Fourier space, that one gets [78]

$$\mathcal{G}^{I}_{(a,\lambda);(a',\lambda')}(\omega) = -i\omega \mathcal{G}_{(a,\lambda);(a',\lambda')}(\omega) - i \langle [I_{a,\lambda}(t), Q_{a',\lambda'}(t)] \rangle = -i\omega \mathcal{G}_{(a,\lambda);(a',\lambda')}(\omega) + \mathcal{G}^{I}_{(a,\lambda);(a',\lambda')}(\omega = 0), \tag{A9}$$

with the last term at the second line of Eq. (A9) being, in fact, independent of t and working to cancel the $\omega = 0$ contribution to the left-hand side.

From the definition of the charge operators $Q_{a,\lambda}$, it is straightforward to derive the explicit formulas for the current operators for the lattice model Hamiltonian in Eq. (A1). In particular, one obtains

$$\begin{aligned} I_{1,<} &= -\frac{ieJ}{2} \{ [c^{\dagger}_{1,1} - c^{\dagger}_{-1,1}] c_{0,1} - c^{\dagger}_{0,1} [c_{1,1} - c_{-1,1}] \} - ieV_{od} \{ c^{\dagger}_{0,1} c_{0,2} - c^{\dagger}_{0,2} c_{0,1} \}, \\ I_{2,<} &= -\frac{ieJ}{2} \{ [c^{\dagger}_{1,2} - c^{\dagger}_{-1,2}] c_{0,2} - c^{\dagger}_{0,2} [c_{1,2} - c_{-1,2}] \} + ieV_{od} \{ c^{\dagger}_{0,1} c_{0,2} - c^{\dagger}_{0,2} c_{0,1} \}, \end{aligned}$$

$$I_{1,>} = \frac{ieJ}{2}\{[c^\dagger_{1,1} - c^\dagger_{-1,1}]c_{0,1} - c^\dagger_{0,1}[c_{1,1} - c_{-1,1}]\} - ieV_{od}\{c^\dagger_{0,1}c_{0,2} - c^\dagger_{0,2}c_{0,1}\},$$
$$I_{2,>} = \frac{ieJ}{2}\{[c^\dagger_{1,2'} - c^\dagger_{-1,2}]c_{0,2} - c^\dagger_{0,2}[c_{1,2} - c_{-1,2}]\} + ieV_{od}\{c^\dagger_{0,1}c_{0,2} - c^\dagger_{0,2}c_{0,1}\}. \tag{A10}$$

To perform the explicit calculation of the ac conductance tensor, we resort to the expansion of the lattice field operators entering Eq. (A1) in terms of chiral fermionic fields reviewed in Eq. (27). This eventually leads to the continuum version of the system Hamiltonian $H_{\rm PL}$, given by

$$H_{\rm PL} = -iv\sum_{a=1,2}\int_{-\ell}^{\ell} dx\,\{\psi^\dagger_{R,a}(x)\partial_x\psi_{R,a}(x) - \psi^\dagger_{L,a}(x)\partial_x\psi_{L,a}(x)\} + V_d\sum_{a=1,2}[\psi^\dagger_{R,a}(0) + \psi^\dagger_{L,a}(0)][\psi_{R,a}(0)$$
$$+ \psi_{L,a}(0)] + V_{od}\{[\psi^\dagger_{R,1}(0) + \psi^\dagger_{L,1}(0)][\psi_{R,2}(0) + \psi_{L,2}(0)] + \text{H.c.}\}. \tag{A11}$$

Also, in terms of the continuum fields, Eqs. (A10) become

$$I_{1,<} = ev\{\psi^\dagger_{R,1}(0)\psi_{R,1}(0) - \psi^\dagger_{L,1}(0)\psi_{L,1}(0)\} - ieV_{od}\{[\psi^\dagger_{R,1}(0) + \psi^\dagger_{L,1}(0)][\psi_{R,2}(0) + \psi_{L,2}(0)] - \text{H.c.}\},$$
$$I_{2,<} = ev\{\psi^\dagger_{R,2}(0)\psi_{R,2}(0) - \psi^\dagger_{L,2}(0)\psi_{L,2}(0)\} + ieV_{od}\{[\psi^\dagger_{R,1}(0) + \psi^\dagger_{L,1}(0)][\psi_{R,2}(0) + \psi_{L,2}(0)] - \text{H.c.}\},$$
$$I_{1,>} = -ev\{\psi^\dagger_{R,1}(0)\psi_{R,1}(0) - \psi^\dagger_{L,1}(0)\psi_{L,1}(0)\} - ieV_{od}\{[\psi^\dagger_{R,1}(0) + \psi^\dagger_{L,1}(0)][\psi_{R,2}(0) + \psi_{L,2}(0)] - \text{H.c.}\},$$
$$I_{2,>} = -ev\{\psi^\dagger_{R,2}(0)\psi_{R,2}(0) - \psi^\dagger_{L,2}(0)\psi_{L,2}(0)\} + ieV_{od}\{[\psi^\dagger_{R,1}(0) + \psi^\dagger_{L,1}(0)][\psi_{R,2}(0) + \psi_{L,2}(0)] - \text{H.c.}\}. \tag{A12}$$

To further simplify the calculations, we now switch to the chiral fermionic fields $\psi_{e,a}(x)$, $\psi_{o,a}(x)$ defined in Eq. (29) of the main text. As stated before, $\psi_{o,1}(x)$ and $\psi_{o,2}(x)$ fully decouple from H_B and, accordingly, they behave as free chiral fermionic fields over a segment of length 2ℓ. The dynamics of $\psi_{e,1}(x)$, $\psi_{e,2}(x)$ is instead described by the Hamiltonian

$$H_e = -iv\int_{-\ell}^{\ell} dx\sum_{a=1,2}\psi^\dagger_{e,a}(x)\partial_x\psi_{e,a}(x) + 2V_d\sum_{a=1,2}\psi^\dagger_{e,a}(0)\psi_{e,a}(0) + 2V_{od}\{\psi^\dagger_{e,1}(0)\psi_{e,2}(0) + \text{H.c.}\}. \tag{A13}$$

At the same time, the current density operators in Eqs. (A12) become

$$I_{1,<} = ev\{\psi^\dagger_{e,1}(0)\psi_{o,1}(0) + \psi^\dagger_{o,1}(0)\psi_{e,1}(0)\} - 2ieV_{od}\{[\psi^\dagger_{e,1}(0)\psi_{e,2}(0) - \psi^\dagger_{e,2}(0)\psi_{e,1}(0)\},$$
$$I_{2,<} = ev\{\psi^\dagger_{e,2}(0)\psi_{o,2}(0) + \psi^\dagger_{o,2}(0)\psi_{e,2}(0)\} + 2ieV_{od}\{[\psi^\dagger_{e,1}(0)\psi_{e,2}(0) - \psi^\dagger_{e,2}(0)\psi_{e,1}(0)\},$$
$$I_{1,>} = -ev\{\psi^\dagger_{e,1}(0)\psi_{o,1}(0) + \psi^\dagger_{o,1}(0)\psi_{e,1}(0)\} - 2ieV_{od}\{[\psi^\dagger_{e,1}(0)\psi_{e,2}(0) - \psi^\dagger_{e,2}(0)\psi_{e,1}(0)\},$$
$$I_{2,>} = -ev\{\psi^\dagger_{e,2}(0)\psi_{o,2}(0) + \psi^\dagger_{o,2}(0)\psi_{e,2}(0)\} + 2ieV_{od}\{[\psi^\dagger_{e,1}(0)\psi_{e,2}(0) - \psi^\dagger_{e,2}(0)\psi_{e,1}(0)\}. \tag{A14}$$

A generic eigenmode of H_e with energy eigenvalue ϵ is written in the form

$$\Gamma_{\epsilon,e} = \sum_{a=1,2}\int_{-\ell}^{\ell} dx\,u^*_{e,a,\epsilon}(x)\psi_{e,a}(x). \tag{A15}$$

On imposing the commutation relation $[\Gamma_{\epsilon,e}, H_e] = \epsilon\Gamma_{\epsilon,e}$, one obtains the Schrödinger equations for the corresponding wave functions in the form

$$\epsilon u_{e,1,\epsilon}(x) = -iv\partial_x u_{e,1,\epsilon}(x) + \delta(x)\{2V_d u_{e,1,\epsilon}(x) + 2V_{od}u_{e,2,\epsilon}(x)\},$$
$$\epsilon u_{e,2,\epsilon}(x) = -iv\partial_x u_{e,2,\epsilon}(x) + \delta(x)\{2V_d u_{e,2,\epsilon}(x) + 2V_{od}u_{e,1,\epsilon}(x)\}. \tag{A16}$$

By explicitly solving Eqs. (A16), one readily finds that the fields $\psi_{e,1}(0)$, $\psi_{e,2}(0)$ at time t can be fully expressed in terms of two sets of anticommuting energy eigenmodes $\{\Gamma_{\epsilon,e,\alpha}, \Gamma_{\epsilon,e,\beta}\}$, as

$$\psi_{e,1}(-vt) = \frac{1}{\sqrt{2\ell}}\sum_\epsilon e^{i\frac{\epsilon x}{v}}\frac{1}{2}\{[1+t_d]\Gamma_{\epsilon,e,\alpha} + t_{od}\Gamma_{\epsilon,e,\beta}\}\,e^{-i\epsilon t},$$
$$\psi_{e,2}(-vt) = \frac{1}{\sqrt{2\ell}}\sum_\epsilon e^{i\frac{\epsilon x}{v}}\frac{1}{2}\{t_{od}\Gamma_{\epsilon,e,\alpha} + [1+t_d]\Gamma_{\epsilon,e,\beta}\}\,e^{-i\epsilon t}, \tag{A17}$$

with

$$t_d = \frac{v^2 - V_{od}^2 + V_d^2}{(v+iV_d)^2 + V_{od}^2}, \quad t_{od} = \frac{-2ivV_{od}}{(v+iV_d)^2 + V_{od}^2}. \tag{A18}$$

To compute the ac conductance tensor, we need the following retarded Green's functions:

$$\mathcal{G}_a(t-t') = -ie^2v^2\theta(t-t')\langle[\psi^\dagger_{e,a}(-vt)\psi_{o,a}(-vt)+\psi^\dagger_{o,a}(-vt)\psi_{e,a}(-vt),\,\psi^\dagger_{e,a}(-vt')\psi_{o,a}(-vt')+\psi^\dagger_{o,a}(-vt')\psi_{e,a}(-vt')]\rangle,$$
$$\mathcal{G}_{od}(t-t') = 4ie^2V^2_{od}\,\langle[\psi^\dagger_{e,1}(-vt)\psi_{e,2}(-vt)-\psi^\dagger_{e,2}(-vt)\psi_{e,1}(-vt),\,\psi^\dagger_{e,1}(-vt')\psi_{e,2}(-vt')-\psi^\dagger_{e,2}(-vt')\psi_{e,1}(-vt')]\rangle. \quad \text{(A19)}$$

Based on the previous derivation, it is simple to explicitly compute the Fourier transform of the functions in Eqs. (A19). In particular, one obtains

$$\mathcal{G}_a(\omega) = -\frac{ie^2}{4\pi}\,[1+\mathrm{Re}(t_d)]\omega = -\frac{i\omega e^2}{2\pi}\left\{\frac{v^2\left[v^2+V_d^2+V_{od}^2\right]}{\left(v^2+V_{od}^2\right)^2+2V_d^2\left(v^2-V_{od}^2\right)+V_d^4}\right\},$$
$$\mathcal{G}_{od}(\omega) = -\frac{i\omega e^2}{2\pi}\left\{\frac{2v^2V_{od}^2}{\left(v^2+V_{od}^2\right)^2+2V_d^2\left(v^2-V_{od}^2\right)+V_d^4}\right\}. \quad \text{(A20)}$$

In the $V_{od}\to 0$ limit (which is relevant for the following derivation), we obtain $\mathbf{G}_{(2,>);(1,<)}(\omega)=0$, while

$$\mathbf{G}_{(1,>);(1,<)}(\omega) = -\frac{e^2}{2\pi}\,\cos^2(\delta_S), \quad \text{(A21)}$$

with

$$\cos(\delta_S) = \frac{v}{\sqrt{v^2+V_d^2}}. \quad \text{(A22)}$$

APPENDIX B: SCHRIEFFER-WOLFF TRANSFORMATION AND DERIVATION OF THE EFFECTIVE KONDO HAMILTONIAN

In general, the SW procedure, when applied to a generic Hamiltonian $\hat{H}$, allows for recovering a reduced, effective Hamiltonian, acting on a limited subspace of the Hilbert space, typically determined as the subspace spanned by a certain set of low-lying eigenstates of $\hat{H}$. To be specific, let us consider a generic time-independent Schrödinger equation

$$\hat{H}|\Psi\rangle = E|\Psi\rangle, \quad \text{(B1)}$$

and suppose we want to "project" it onto a pertinently defined low-energy subspace $\mathbf{G}$. Let $\mathcal{P}_\mathbf{G}$ be the projector on $\mathbf{G}$. To lowest order in the "off-diagonal" matrix elements connecting $\mathbf{G}$ to its orthogonal subspace, we obtain

$$\mathcal{P}_\mathbf{G}\hat{H}\mathcal{P}_\mathbf{G}\{\mathcal{P}_\mathbf{G}|\Psi\rangle\}+\mathcal{P}_\mathbf{G}\hat{H}[\mathbf{I}-\mathcal{P}_\mathbf{G}]\{[\mathbf{I}-\mathcal{P}_\mathbf{G}]|\Psi\rangle\} = E\{\mathcal{P}_\mathbf{G}|\Psi\rangle\},$$
$$[\mathbf{I}-\mathcal{P}_\mathbf{G}]\hat{H}[\mathbf{I}-\mathcal{P}_\mathbf{G}]\{\mathcal{P}_\mathbf{G}|\Psi\rangle\}+[\mathbf{I}-\mathcal{P}_\mathbf{G}]\hat{H}\mathcal{P}_\mathbf{G}\{\mathcal{P}_\mathbf{G}|\Psi\rangle\} = E\{[\mathbf{I}-\mathcal{P}_\mathbf{G}]|\Psi\rangle\}. \quad \text{(B2)}$$

Putting together Eqs. (B2), one eventually obtains the "projected" Schrödinger equation

$$\{\mathcal{P}_\mathbf{G}\hat{H}\mathcal{P}_\mathbf{G}+\mathcal{P}_\mathbf{G}\hat{H}[\mathbf{I}-\mathcal{P}_\mathbf{G}][E-[\mathbf{I}-\mathcal{P}_\mathbf{G}]\hat{H}[\mathbf{I}-\mathcal{P}_\mathbf{G}]]^{-1}[\mathbf{I}-\mathcal{P}_\mathbf{G}]\hat{H}\mathcal{P}_\mathbf{G}\}\mathcal{P}_\mathbf{G}|\Psi\rangle = E\mathcal{P}_\mathbf{G}|\Psi\rangle. \quad \text{(B3)}$$

Dividing the Hamiltonian as the sum of a nonperturbed contribution plus a perturbation term $H=H_0+H_1$, we can project it onto the (n times degenerate) ground-state subspace of H_0:

$$H_0|\psi_i\rangle = E_{0,i}|\psi_i\rangle, \quad i=1,\ldots,n \quad \text{(B4)}$$

to obtain the Brillouin-Wigner perturbation expansion

$$H_{\mathrm{Eff}} = \sum_{i,j} h_{i,j}|\psi_i\rangle\langle\psi_j| \quad \text{(B5)}$$

with

$$h_{i,j} = \langle\psi_i|H_0|\psi_j\rangle+\langle\psi_i|H_1|\psi_j\rangle+\sum_k\frac{\langle\psi_i|H_1|\varphi_k\rangle\langle\varphi_k|H_1|\psi_j\rangle}{E_0-E_k}, \quad \text{(B6)}$$

where the sum over k runs on the low-energy excited states of the unperturbed Hamiltonian. Equations (B1) and (B2) define a systematic procedure. A straightforward implementation of the procedure we illustrate here allows for recovering the effective Kondo Hamiltonians in Eqs. (16) and (18).

Another effective use of the SW transformation leads to the residual interaction at both the SK and CK fixed points. To illustrate our derivation, we consider the SK fixed point. For the sake of generality, we consider an anisotropic lattice version of

the lattice SK model Hamiltonian in the form

$$H_{\mathrm{Lat;S}} = \sum_{a=1,2} \left\{ -J \sum_{j=-\ell}^{\ell-1} [c^\dagger_{j,a} c_{j+1,a} + c^\dagger_{j+1,a} c_{j,a}] - \mu \sum_{j=-\ell}^{\ell} c^\dagger_{j,a} c_{j,a} \right\} + J_{S,\perp} \{S_0^+ \mathcal{S}^- + S_0^- \mathcal{S}^+\} + J_{S,z} S_0^z \mathcal{S}_1^z. \tag{B7}$$

The ground state at the SK fixed point minimizes the boundary interaction energy encoded in the Hamiltonian in Eq. (B7) as $J_{S,\perp}, J_{S,z} \to \infty$. To explicitly provide such a state, in the following, we denote by $|\Uparrow\rangle, |\Downarrow\rangle$ the two eigenstates of $\mathcal{S}^z$, with $|0\rangle, |\uparrow\rangle, |\downarrow\rangle, |\downarrow\uparrow\rangle$ the states in which, respectively, the site $j = 0$ is empty in both chains is filled with one electron on chain 1 and empty on chain 2, is filled with one electron on chain 2 and empty on chain 1, is filled with one electron in both chains. As a result of the hybridization with the impurity spin, the locally hybridized states, which we list below together with the corresponding energies, are generated:

$$\begin{aligned}
&\text{Local singlet}: \ |S\rangle = \frac{1}{\sqrt{2}} \{|\downarrow, \Uparrow\rangle - |\uparrow, \Downarrow\rangle\}; \ \left(\epsilon_S = -\frac{1}{4}(S_{S,z} + 2J_{S,\perp})\right), \\
&\text{Local doublet } D: \ |D_\sigma\rangle = |0, \sigma\rangle; \ (\epsilon_D = 0), \\
&\text{Local doublet } \tilde{D}: \ |\tilde{D}_\sigma\rangle = |\downarrow\uparrow, \sigma\rangle; \ (\epsilon_{\tilde{D}} = 0), \\
&\text{Local triplet } T_1: \ |T_1\rangle = |\uparrow, \Uparrow\rangle; \ \left(\epsilon_{T,1} = \frac{J_{S,z}}{4}\right), \\
&\text{Local triplet } T_{-1}: \ |T_{-1}\rangle = |\downarrow, \Downarrow\rangle; \ \left(\epsilon_{T,-1} = \frac{J_{S,z}}{4}\right), \\
&\text{Local triplet } T_0: \ |T_0\rangle = \frac{1}{\sqrt{2}} \{|\downarrow, \Uparrow\rangle + |\uparrow, \Downarrow\rangle\}; \ \left(\epsilon_{T,0} = \frac{1}{4}(-J_{S,z} + 2J_{S,\perp})\right).
\end{aligned} \tag{B8}$$

At large values of $J_{S,\perp}, J_{S,z}$, the system lies within the $|S\rangle$ local state, with the higher-energy states in Eqs. (B8) playing a role in the allowed physical processes only as virtual states. Taking this into account, one can therefore go through a systematic SW transformation, by using as "unperturbed" Hamiltonian $\mathcal{H}_0 = \sum_X \epsilon_X |X\rangle\langle X|$, with $\{|X\rangle\}$ being the set of states listed in Eqs. (B8), and as "perturbing" Hamiltonian $\mathcal{H}_t$, describing the coupling between site 0 and sites -±1 of each lead, and given by

$$\mathcal{H}_t = t\{[c_{1,1} + c_{-1,1}]c^\dagger_{0,1} + [c_{1,2} + c_{-1,2}]c^\dagger_{0,2} - [c^\dagger_{1,1} + c^\dagger_{-1,1}]c_{0,1} - [c^\dagger_{1,2} + c^\dagger_{-1,2}]c_{0,2}\}. \tag{B9}$$

As a result, one finds that the first nontrivial boundary interaction operator $\tilde{H}_{K,S}$ arises to fourth order in $\mathcal{H}_t$, and is given by

$$\tilde{H}_{K,S} = \sum_{\{X,X'\}=\{D_\sigma,\tilde{D}_\sigma\}} \sum_{\{Y\}=\{T_M\}} \left[\mathcal{P}_S \frac{\mathcal{H}_t}{\epsilon_S - \epsilon_X} \mathcal{P}_X \frac{\mathcal{H}_t}{\epsilon_S - \epsilon_Y} \mathcal{P}_Y \frac{\mathcal{H}_t}{\epsilon_S - \epsilon_{X'}} \mathcal{P}_{X'} \mathcal{H}_t \mathcal{P}_S \right], \tag{B10}$$

with $\mathcal{P}_X$ being the projector onto the space spanned by the local state $|X\rangle$. Plugging into Eq. (B10) the explicit expressions for $\mathcal{H}_t$ and for the various energies, one finds

$$\begin{aligned}
\tilde{H}_{K,S} = &-\zeta_{I,\perp}\{[(c_{1,2} + c_{-1,2}), (c^\dagger_{1,1} + c_{-1,1})][(c_{1,1} + c_{-1,1}), (c^\dagger_{1,2} + c^\dagger_{-1,2})] \\
&+ [(c_{1,1} + c_{-1,1}), (c^\dagger_{1,2} + c^\dagger_{-1,2})][(c_{1,2} + c_{-1,2}), (c^\dagger_{1,1} + c_{-1,1})]\} \\
&- \zeta_{I,z}\{[(c_{1,2} + c_{-1,2}), (c^\dagger_{1,2} + c^\dagger_{-1,2})] - [(c_{1,1} + c_{-1,1}), (c^\dagger_{1,1} + c^\dagger_{-1,1})]\}^2,
\end{aligned} \tag{B11}$$

with

$$\zeta_{I,\perp} = \frac{t^4}{4\epsilon_S^2[\epsilon_{T_1} - \epsilon_S]}, \quad \zeta_{I,z} = \frac{t^4}{4\epsilon_S^2[\epsilon_{T_0} - \epsilon_S]}. \tag{B12}$$

$\tilde{H}_{K,S}$ in Eq. (B11) is the lattice version of the operator describing the leading perturbation at Nozières Fermi-liquid fixed point as derived in, e.g., Appendix D of Ref. [6]. Resorting to the continuum field framework by means of, e.g., the low-energy, long-wavelength expansions in Eqs. (28) and (29) and inserting the continuum fields, supplemented with the appropriate fixed-point boundary conditions, in Eq. (B12), one recovers the continuum formula for the leading boundary perturbation at the SK fixed point [Eq. (35)]. Similarly, at the CK fixed point, one obtains Eq. (38) of the main text.

APPENDIX C: DERIVATION OF H_{DL} IN THE DISCONNECTED LEAD PHASE

In this Appendix, we briefly discuss the derivation of H_{DL} in Eq. (26) as the leading boundary interaction describing the impurity within the DL phase. To do so, we start by "artificially" introducing two independent parameters in the DSI Hamiltonian,

which we accordingly rewrite as

$$\hat{H}_{\rm Island} = -2\delta_1 \sum_{a=1,2} a_a^\dagger a_a + 4\delta_2 a_1^\dagger a_1 a_2^\dagger a_2. \tag{C1}$$

Clearly, in order to recover physically meaningful results, one has to eventually set $\delta_1 = \delta_2 = \delta$. However, Eq. (C1) comes out to be useful in that it allows for exactly accounting for at least part of the δ-depending terms in $H_{\rm Island}$.

Identifying δ_2 as our perturbative parameter, we note that, leaving aside the density-density interaction (that is, setting $\mu_{\rm d} = \mu_{\rm od} = 0$), the system Hamiltonian can be written as $\hat{H}_0 = \sum_{a=1,2} \hat{H}_a$, with

$$\hat{H}_a = -J \sum_{j=-\ell}^{\ell-1} \{c_{j,a}^\dagger c_{j+1,a} + c_{j+1,a}^\dagger c_{j,a}\} - \mu \sum_{j=-\ell}^{\ell} c_{j,a}^\dagger c_{j,a} - t\{c_{0,a}^\dagger a_a + a_a^\dagger c_{0,a}\} - 2\delta_1 a_a^\dagger a_a. \tag{C2}$$

The right-hand side of Eq. (C2) contains a quadratic Hamiltonian defined over an $(2\ell + 2)$-site lattice. This can be exactly diagonalized by means of the eigenmodes $\Gamma_{k,a}$, defined as

$$\Gamma_{k,a} = \sum_{j=-\ell}^{\ell} u_{j,a,k} c_{j,a} + \xi_{k,a} a_a, \tag{C3}$$

and (on imposing periodic boundary conditions at $j = \pm\ell$) the wave functions satisfying the lattice Schrödinger equation

$$\begin{aligned} \epsilon_k u_{j,k,a} &= -J\{u_{j+1,k,a} + u_{j-1,k,a}\} - \mu u_{j,k,a} \quad (j \neq 0), \\ \epsilon_k u_{0,k,a} &= -J\{u_{1,k,a} + u_{-1,k,a}\} - \mu u_{0,k,a} - t\xi_{k,a}, \quad \epsilon_k \xi_{k,a} = -2\delta_1 \xi_{k,a} - t u_{0,k,a}. \end{aligned} \tag{C4}$$

To solve Eqs. (C4), we make the ansatz

$$\begin{aligned} u_{j,k,a} &= \alpha_{k,a}^{<} e^{ikj} + \beta_{k,a}^{<} e^{-ikj} \quad (-\ell \leqslant j < 0), \\ u_{j,k,a} &= \alpha_{k,a}^{>} e^{ikj} + \beta_{k,a}^{>} e^{-ikj} \quad (0 < j \leqslant \ell), \end{aligned} \tag{C5}$$

which yields $\epsilon_k = -2J\,\cos(k) - \mu$ and, in addition, the conditions at $j = 0$ encoded in

$$\begin{aligned} u_{0,k,a} &= \alpha_{k,a}^{<} + \beta_{k,a}^{<}, \quad u_{0,k,a} = \alpha_{k,a}^{>} + \beta_{k,a}^{>}, \\ 2J\,\cos(k)\, u_{0,k,a} &= J\{\alpha_{k,a}^{<} e^{-ik} + \beta_{k,a}^{<} e^{ik} + \alpha_{k,a}^{>} e^{ik} + \beta_{k,a}^{>} e^{-ik}\} + t\xi_{k,a}, \\ \{2J\,\cos(k) + \mu - 2\delta_1\}\xi_{k,a} &= t u_{0,k,a}. \end{aligned} \tag{C6}$$

Once the system in Eqs. (C6) has been explicitly solved, at a given k, one obtains

$$\begin{aligned} u_{0,k,a} &= \alpha \left\{ -\frac{2iJ(\epsilon_k + 2\delta_1)\sin(k)}{(\epsilon_k + 2\delta_1)(\epsilon_k + \mu) + 2ie^{ik}J(\epsilon_k + 2\delta_1) - t^2} \right\}, \\ \xi_{k,a} &= \alpha \left\{ \frac{2iJt\,\sin(k)}{(\epsilon_k + 2\delta_1)(\epsilon_k + \mu) + 2ie^{ik}J(\epsilon_k + 2\delta_1) - t^2} \right\}, \end{aligned} \tag{C7}$$

with α being an overall normalization constant. Considering specific solutions obeying scattering boundary conditions, such as

$$u_{j,k,a}^{(1)} = \begin{cases} \alpha\left\{e^{ikj} + r_{k,a}^{(1)} e^{-ikj}\right\} & (j < 0), \\ \alpha t_{k,a}^{(1)} e^{ikj} & (j > 0) \end{cases} \tag{C8}$$

and

$$u_{j,k,a}^{(1)} = \begin{cases} \alpha t_{k,a}^{(2)} e^{-ikj} & (j < 0), \\ \alpha\left\{e^{-ikj} + r_{k,a}^{(2)} e^{ikj}\right\} & (j > 0), \end{cases} \tag{C9}$$

one obtains

$$t_{k,a}^{(1)} = t_{k,a}^{(2)} = \left\{ -\frac{2iJ(\epsilon_k + 2\delta_1)\sin(k)}{(\epsilon_k + 2\delta_1)(\epsilon_k + \mu) + 2ie^{ik}J(\epsilon_k + 2\delta_1) - t^2} \right\}. \tag{C10}$$

At the Fermi level one therefore obtains

$$t^{(1)}_{k_F,a} = t^{(2)}_{k_F,a} = \frac{2i\delta_1 v}{2i\delta_1 v - t^2}, \tag{C11}$$

with v being the Fermi velocity. Also, given the relations

$$c_{0,a} = \sum_k u^*_{0,k,a}\Gamma_{k,a}, \quad a_a = \sum_k \xi^*_{k,a}\Gamma_{k,a}, \tag{C12}$$

one notes that, approximating $t^{(1,2)}_{k,a}$ with $t^{(1,2)}_{k_F,a}$ in Eq. (C11) (which clearly applies to energy scales lower than $|t|$) and if $\delta_1 \neq 0$, one obtains

$$a_a \approx -\frac{t}{2\delta_1}c_{0,a} \Rightarrow a^\dagger_a a_a \approx \frac{t^2}{4\delta_1^2}c^\dagger_{0,a}c_{0,a}. \tag{C13}$$

Equation (C13) implies $a^\dagger_a a_a \propto c^\dagger_{0,a}c_{0,a}$. Therefore, the whole impurity interaction Hamiltonian can be traded for a density-density interaction one, $H_{\rm DL}$, of the form

$$H_{\rm DL} = \kappa c^\dagger_{0,1}c_{0,1}c^\dagger_{0,2}c_{0,2} + \sum_{a=1,2}\lambda_a c^\dagger_{0,a}c_{0,a}, \tag{C14}$$

with $\kappa, \lambda_1, \lambda_2$ parameters corresponding to the interwire local density-density interaction and to the residual intrawire local one-body potentials and $\kappa \approx (\frac{t}{2\delta_1})^4\,\delta_2$. $H_{\rm DL}$ in Eq. (C14) is the Hamiltonian we used in the main text to discuss the effective impurity dynamics in the DL region of the phase diagram.

APPENDIX D: RENORMALIZATION GROUP EQUATIONS FOR THE RUNNING COUPLING IN THE EFFECTIVE IMPURITY HAMILTONIANS

In this Appendix, we concisely review the derivation and the solution of the RG equations for the various boundary Hamiltonians describing the impurity dynamics in the various regions of the system. To begin with, we consider $\hat{H}_{\rm K,S}$ in Eq. (20) and $\hat{H}_{\rm K,C}$ in Eq. (21). For the sake of the discussion, here we leave aside purely marginal terms (that is, one-body potential scattering terms), whose nonuniversal effects we account for when actually computing the dc conductance tensor of the system. At the same time, we neglect local fields acting on the effective spin impurity, whose effects we briefly discuss by the end of this Appendix. Accordingly, in order to encompass in our analysis both cases, we henceforth consider the RG equations for the running couplings associated a generic anisotropic Kondo Hamiltonian $H_{\rm An}$, given by

$$H_{\rm An} = J_\perp\{\psi^\dagger_1(0)\psi_2(0)\mathcal{S}^- + \psi^\dagger_2(0)\psi_1(0)\mathcal{S}^+\} + J_z\left\{\frac{\psi^\dagger_1(0)\psi_1(0) - \psi^\dagger_2(0)\psi_2(0)}{2}\right\}\mathcal{S}^z, \tag{D1}$$

with $\psi_1(x), \psi_2(x)$ being one-dimensional, chiral fermionic fields. $J_\perp$ and J_z are, respectively, the transverse and the longitudinal Kondo coupling strengths. On defining the associated dimensionless running coupling strengths $\mathcal{J}_\perp(D) = \frac{aJ_\perp}{v}$ and $\mathcal{J}_z(D) = \frac{aJ_z}{v}$, the derivation of the RG equations for those running coupling has a long story and goes back to the original works on the subject [2,79–81]. Specifically, on varying the energy cutoff D, one obtains that the corresponding variation of the running couplings is determined by the equations

$$\frac{d\mathcal{J}_\perp(D)}{d\,\ln\left(\frac{D_0}{D}\right)} = \mathcal{J}_\perp(D)\mathcal{J}_z(D), \quad \frac{d\mathcal{J}_z(D)}{d\,\ln\left(\frac{D_0}{D}\right)} = \mathcal{J}^2_\perp(D). \tag{D2}$$

The system in Eqs. (D2) corresponds to the set of the standard Kosterlitz-Thouless RG equations. To solve it, one defines the RG invariant $H = -\mathcal{J}^2_z(D) + \mathcal{J}^2_\perp(D)$. In particular, for $H = 0$, one recovers the standard poor man's result for the RG equations in the case of isotropic Kondo effect [2,81]. In this case, one readily finds the solution in the form

$$\mathcal{J}_\perp(D) = \mathcal{J}_\parallel(D) = \frac{\mathcal{J}_\perp(D_0)}{1 - \mathcal{J}_\perp(D_0)\ln\left(\frac{D_0}{D}\right)}, \tag{D3}$$

with the corresponding Kondo scale $D_K(= kT_K)$ given by

$$D_K \sim D_0 e^{-\frac{1}{\mathcal{J}_\perp(D_0)}}. \tag{D4}$$

At a generic value of H, as we show in Fig. 6 there are three relevant regions in the half-plane $\mathcal{J}_z, \mathcal{J}_\perp > 0$. In detail, we have the following:

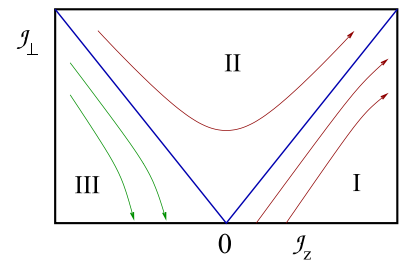

FIG. 6. Sketch of the RG trajectories for the running couplings $\mathcal{J}_\perp(D)$ and $\mathcal{J}_z(D)$.

(i) *Region I*: This is defined for $\mathcal{J}_\parallel(D_0) > 0$ and $H < 0$. In this case, the integrated RG equations yield

$$\mathcal{J}_z(D) = \sqrt{|H|}\left\{\frac{\mathcal{J}_z(D_0)+\sqrt{|H|}+[\mathcal{J}_z(D_0)-\sqrt{|H|}]\left(\frac{D_0}{D}\right)^{2\sqrt{|H|}}}{\mathcal{J}_z(D_0)+\sqrt{|H|}-[\mathcal{J}_z(D_0)-\sqrt{|H|}]\left(\frac{D_0}{D}\right)^{2\sqrt{|H|}}}\right\},$$
$$\mathcal{J}_\perp(D) = 2\sqrt{|H|}\left\{\frac{\sqrt{\mathcal{J}_z^2(D_0)-|H|}\left(\frac{D_0}{D}\right)^{\sqrt{|H|}}}{\mathcal{J}_z(D_0)+\sqrt{|H|}-[\mathcal{J}_z(D_0)-\sqrt{|H|}]\left(\frac{D_0}{D}\right)^{2\sqrt{|H|}}}\right\}. \tag{D5}$$

Both running couplings increase as D_0/D gets large. Eventually, they hit a diverging point at the scale $D = D_{\mathrm{KT}}^{(1)}$, with

$$D_{\mathrm{KT}}^{(1)} = D_0\left\{\frac{\mathcal{J}_z(D_0)-\sqrt{|H|}}{\mathcal{J}_z(D_0)+\sqrt{|H|}}\right\}^{\frac{1}{2\sqrt{|H|}}}. \tag{D6}$$

(ii) *Region II*: This is defined for $H > 0$. In this case, one obtains

$$\mathcal{J}_z(D) = \sqrt{H}\,\tan\left\{\mathrm{atan}\left(\frac{\mathcal{J}_z(D_0)}{\sqrt{H}}\right)+\sqrt{H}\ln\left(\frac{D_0}{D}\right)\right\},\quad \mathcal{J}_\perp(D) = \frac{\sqrt{H}}{\cos\left\{\mathrm{atan}\left(\frac{\mathcal{J}_z(D_0)}{\sqrt{H}}\right)+\sqrt{H}\ln\left(\frac{D_0}{D}\right)\right\}}. \tag{D7}$$

In the case $G_z(D_0) < 0$, Eqs. (D7) imply a crossing of the vertical axis at the scale D_{cross} defined as

$$D_{\mathrm{cross}} = D_0\exp\left[-\frac{1}{\sqrt{H}}\left|\mathrm{atan}\left(\frac{\mathcal{J}_z(D_0)}{\sqrt{H}}\right)\right|\right]. \tag{D8}$$

Both couplings diverge at the scale $D = D_{\mathrm{KT}}^{(2)}$, with

$$D_{\mathrm{KT}}^{(2)} = D_0\exp\left\{-\frac{1}{\sqrt{H}}\left[\frac{\pi}{2}-\mathrm{atan}\left(\frac{\mathcal{J}_z(D_0)}{\sqrt{H}}\right)\right]\right\}. \tag{D9}$$

(iii) *Region III:* This is defined for $\mathcal{J}_z(D_0) < 0$ and $H < 0$. In this case, the integrated RG trajectory take the form

$$\mathcal{J}_z(D) = \sqrt{|H|}\left\{\frac{|\mathcal{J}_z(D_0)|-\sqrt{|H|}+[|\mathcal{J}_z(D_0)|+\sqrt{|H|}]\left(\frac{D_0}{D}\right)^{2\sqrt{|H|}}}{|\mathcal{J}_z(D_0)|-\sqrt{|H|}-[|\mathcal{J}_z(D_0)|+\sqrt{|H|}]\left(\frac{D_0}{D}\right)^{2\sqrt{|H|}}}\right\},$$
$$\mathcal{J}_\perp(D) = 2\sqrt{|H|}\left\{\frac{\sqrt{\mathcal{J}_z^2(D_0)-|H|}\left(\frac{D_0}{D}\right)^{\sqrt{|H|}}}{-|\mathcal{J}_z(D_0)|+\sqrt{|H|}+[|\mathcal{J}_z(D_0)|+\sqrt{|H|}]\left(\frac{D_0}{D}\right)^{2\sqrt{|H|}}}\right\}. \tag{D10}$$

In this case, we see that the flow is no more toward a point at ∞, but we rather get

$$\lim_{\frac{D_0}{D}\to\infty}\begin{bmatrix}\mathcal{J}_z(D)\\ \mathcal{J}_\perp(D)\end{bmatrix} = \begin{bmatrix}-\sqrt{|H|}\\ 0\end{bmatrix}. \tag{D11}$$

From the analysis we perform above, it is natural to associate the onset of the Kondo regime (and the corresponding emergence of a dynamically generated energy scale) to regions I and II, while region III is characterized by a flow toward a manifold of "trivial" fixed points, continuously parametrized by H. In Fig. 6 we provide a sketch of the RG trajectories for $\mathcal{J}_\perp(D)$ and $\mathcal{J}_z(D)$ by particularly evidencing how, in the "Kondo regions" I and II, both running couplings flow to ∞. While this result is important for building a description of the corresponding Kondo fixed point, we now briefly review what are the possible effects of the "non-Kondo" terms in Eqs. (20) and (21).

A first additional term potentially appearing in the Kondo boundary Hamiltonian is the one-body, local scattering potential, which may just marginally change the single-particle phase shifts at the impurity location and, correspondingly, slightly renormalize the ac conductance tensor with the Kondo interaction turned off, without essentially affecting the Kondo physics [2]. Also, in the CK regime, one may get a term corresponding to an effective, local magnetic field along the z direction, either coupled to the impurity spin, or to the electronic spin density at the impurity location (or both). In general, these terms are known not to substantially affect the Kondo physics as long as the applied field B is much lower than the energy scale associated to the Kondo temperature [17,72,73]. In fact, this is the assumption we make here, as the effective B field is determined by the direct density-density interaction within the wires, which is expected to be much lower than the other energy scales in the system. Therefore, throughout all this paper, we consistently neglect the corresponding contributions to the boundary Hamiltonian effectively describing the impurity dynamics.

To conclude the discussion of this Appendix, we now consider H_{DL} in Eq. (26). Aside from the one-body local

scattering potentials, the only nontrivial interaction term is the direct local density-density coupling, $\propto\kappa$. To deal with it, we therefore introduce the corresponding running coupling $\mathcal{K}(D) = (\frac{D_0}{D})^{-1}\kappa$. The RG equation for $\mathcal{K}(D)$ to leading order in the running coupling is therefore given by

$$\frac{d\mathcal{K}(D)}{d\,\ln\left(\frac{D_0}{D}\right)} = -\mathcal{K}(D), \tag{D12}$$

which shows that this term is irrelevant and that, on lowering the cutoff, the corresponding running coupling scales as D/D_0. Accordingly, its effects can be consistently accounted for within a standard perturbative analysis in the coupling itself, which is what we made when, e.g., discussing the effects of $H_{\rm DL}$ on the dc conductance tensor of the system.

APPENDIX E: AC CONDUCTANCE TENSOR: DETAILS ABOUT THE DERIVATION IN THE VARIOUS REGIONS OF THE PHASE DIAGRAM OF THE SYSTEM

In this Appendix, we explicitly compute the equilibrium ac conductance tensor in the various phases of our system. To do so, we resort to a perturbative expansion around the fixed point corresponding to each one of the phases. When required by the onset of a nonperturbative regime triggered by Kondo interaction, we pertinently complement our analysis within renormalization group framework. In doing so, we assume that ac frequency ω is large enough, so to avoid the suppression of the conductance determined by the emergence of the finite timescale ("Korringa time" τ_K [78]), characterizing correlations between subsequent impurity spin flips. Indeed, at frequencies $\omega \leqslant \tau_K^{-1}$, the spin conductance across the impurity (which, in our case, corresponds to the interwire conductance) is suppressed to 0 [78,82–84]. Thus, in the following derivation we assume that the condition $\omega, kT_K \gg kT$ always holds, so that, as discussed below τ_K can be safely neglected and the perturbative calculation scheme applies [78,83].

To encompass the various regimes of our system addressed in the paper, in the following we separately discuss the calculation for the effective spin and charge Kondo models, as well as for the DL limit (which, in view of the apparent similarity between the corresponding boundary perturbations at the impurity, is expected to describe equally well the system in the vicinity of the spin and of the charge Kondo fixed points).

1. Calculation of the ac conductance tensor in the Kondo regime

According to the derivation of Appendix A, we begin by defining the analogs of Eqs. (A14) in our case:

(i) For the spin Kondo effective model

$$\begin{aligned}
I_{1,<} &= ev\{\psi^\dagger_{e,1}(0)\psi_{o,1}(0) + \psi^\dagger_{o,1}(0)\psi_{e,1}(0)\} - \frac{e}{2}\frac{d\mathcal{S}^z}{dt},\\
I_{2,<} &= ev\{\psi^\dagger_{e,2}(0)\psi_{o,2}(0) + \psi^\dagger_{o,2}(0)\psi_{e,2}(0)\} + \frac{e}{2}\frac{d\mathcal{S}^z}{dt},\\
I_{1,>} &= -ev\{\psi^\dagger_{e,1}(0)\psi_{o,1}(0) + \psi^\dagger_{o,1}(0)\psi_{e,1}(0)\} - \frac{e}{2}\frac{d\mathcal{S}^z}{dt},\\
I_{2,>} &= -ev\{\psi^\dagger_{e,2}(0)\psi_{o,2}(0) + \psi^\dagger_{o,2}(0)\psi_{e,2}(0)\} + \frac{e}{2}\frac{d\mathcal{S}^z}{dt}.
\end{aligned} \tag{E1}$$

(ii) For the charge Kondo effective model

$$\begin{aligned}
I_{1,<} &= ev\{\psi^\dagger_{e,1}(0)\psi_{o,1}(0) + \psi^\dagger_{o,1}(0)\psi_{e,1}(0)\} - \frac{e}{2}\frac{d\mathcal{T}^z}{dt},\\
I_{2,<} &= ev\{\psi^\dagger_{e,2}(0)\psi_{o,2}(0) + \psi^\dagger_{o,2}(0)\psi_{e,2}(0)\} - \frac{e}{2}\frac{d\mathcal{T}^z}{dt},\\
I_{1,>} &= -ev\{\psi^\dagger_{e,1}(0)\psi_{o,1}(0) + \psi^\dagger_{o,1}(0)\psi_{e,1}(0)\} - \frac{e}{2}\frac{d\mathcal{T}^z}{dt},\\
I_{2,>} &= -ev\{\psi^\dagger_{e,2}(0)\psi_{o,2}(0) + \psi^\dagger_{o,2}(0)\psi_{e,2}(0)\} - \frac{e}{2}\frac{d\mathcal{T}^z}{dt}.
\end{aligned} \tag{E2}$$

In the SK case, as it emerges from Eqs. (E1), the whole set of current-current correlation functions is determined by the correlations of the three operators $\mathcal{O}_{1;\rm KS}(t)$, $\mathcal{O}_{2;\rm KS}(t)$, $\mathcal{O}_{\rm S;KS}(t)$, given by

$$\begin{aligned}
\mathcal{O}_{1;\rm KS}(t) &= ev\{\psi^\dagger_{e,1}(-vt)\psi_{o,1}(-vt) + \psi^\dagger_{o,1}(-vt)\psi_{e,1}(-vt)\},\\
\mathcal{O}_{2;\rm KS}(t) &= ev\{\psi^\dagger_{e,2}(-vt)\psi_{o,2}(-vt) + \psi^\dagger_{o,2}(-vt)\psi_{e,2}(-vt)\},\\
\mathcal{O}_{\rm S;KS}(t) &= e\frac{d\mathcal{S}^z(t)}{dt}.
\end{aligned} \tag{E3}$$

To simplify the following calculations, we note that, due to the fact that the spin Kondo Hamiltonian only depends on the $\psi_{e,\alpha}$ fields and due to the identity

$$\begin{aligned}
e\frac{d\mathcal{S}^z(t)}{dt} &= 2ieJ_{S,\perp}\{\psi^\dagger_{e,1}(-vt)\psi_{e,2}(-vt)\mathcal{S}^-(t)\\
&\quad - \psi^\dagger_{e,2}(-vt)\psi_{e,1}(-vt)\mathcal{S}^+(t)\},
\end{aligned} \tag{E4}$$

we readily obtain that

$$\mathcal{G}_{(a,\rm S);KS}(t-t') = -i\theta(t-t')\,\langle[\mathcal{O}_{a;\rm KS}(t), \mathcal{O}_{\rm S;KS}(t')]\rangle = 0 \tag{E5}$$

for $a = 1, 2$. By means of analogous arguments, we also obtain

$$\mathcal{G}_{(1,2);\rm KS}(t-t') = -i\theta(t-t')\,\langle[\mathcal{O}_{1;\rm KS}(t), \mathcal{O}_{2;\rm KS}(t')]\rangle = 0 \tag{E6}$$

as well. [Note that Eqs. (E5) and (E6) only depend on the functional form of the operators involved in the calculations. Therefore, they are exact at any order of the perturbative expansion in J_S.] Therefore, we only need to compute "diagonal" correlation functions. Retaining the leading perturbative contributions in $J_{S,\perp}$, we stop our derivation to order $J^2_{S,\perp}$. We therefore obtain

$$\begin{aligned}
\mathcal{G}_{\rm S;KS}(t-t') &= -ie^2\theta(t-t')\left\langle\left[\frac{d\mathcal{S}^z(t)}{dt}, \frac{d\mathcal{S}^z(t')}{dt'}\right]\right\rangle\\
&= -\frac{4ie^2J^2_{S,\perp}}{(2\ell)^2}\,\theta(t-t')\sum_{\epsilon,\epsilon'} f(\epsilon)f(\epsilon')\\
&\quad\times\{e^{i(\epsilon+\epsilon')(t-t')} - e^{-i(\epsilon+\epsilon')(t-t')}\},
\end{aligned} \tag{E7}$$

with $f(\epsilon)$ being Fermi distribution function. When resorting to Fourier space, Eq. (E7) implies

$$\mathcal{G}_{\mathrm{S;KS}}(\omega) = \frac{4e^2 J_{S,\perp}^2}{(2\ell)^2} \sum_{\epsilon,\epsilon'} f(\epsilon) f(\epsilon') \times \left[\frac{1}{\omega + (\epsilon + \epsilon') - i\eta} - \frac{1}{\omega - (\epsilon + \epsilon') - i\eta} \right], \tag{E8}$$

with $\eta = 0^+$. Similarly, one obtains

$$\begin{aligned} &\mathcal{G}_{(a,a);\mathrm{KS}}(\omega) \\ &= -i \int d(t-t')\, e^{i\omega(t-t')}\, \theta(t-t')\, \langle [\mathcal{O}_{a;\mathrm{KS}}(t), \mathcal{O}_{a;\mathrm{KS}}(t')] \rangle \\ &= -\frac{ie^2\omega}{2\pi} \left\{ 1 - \frac{3J_{S,\perp}^2}{v^2} \right\}. \end{aligned} \tag{E9}$$

Equations (E8) and (E9) are all we need to perturbatively compute the ac conductance. As a result, we obtain

$$\begin{aligned} \mathbf{G}_{(1,>);(1,<)}(\omega) &= -\frac{e^2}{2\pi} \left\{ 1 - \frac{J_{S,\perp}^2}{v^2} \right\}, \\ \mathbf{G}_{(2,>);(1,<)}(\omega) &= -\frac{e^2}{2\pi} \frac{J_{S,\perp}^2}{v^2}. \end{aligned} \tag{E10}$$

Similarly, in the charge Kondo case one obtains

$$\begin{aligned} \mathbf{G}_{(1,>);(1,<)}(\omega) &= -\frac{e^2}{2\pi} \left\{ 1 - \frac{J_{C,\perp}^2}{v^2} \right\}, \\ \mathbf{G}_{(2,>);(1,<)}(\omega) &= \frac{e^2}{2\pi} \frac{J_{C,\perp}^2}{v^2}. \end{aligned} \tag{E11}$$

Equations (E10) and (E11) are expected to apply in the frequency range $\omega \gg kT_K$. As ω goes down toward kT_K, one expects that the net effect of the Kondo interaction is to renormalize the coupling strengths $J_{S,\perp}, J_{C,\perp}$ as discussed in Appendix D, with ω corresponding to the running scale D. Taking this into account, Eqs. (E10) and (E11) become

$$\begin{aligned} \mathbf{G}_{(1,>);(1,<)}(\omega) &= -\frac{e^2}{2\pi} \left\{ 1 - \mathcal{J}_{S,\perp}^2(\omega) \right\}, \\ \mathbf{G}_{(2,>);(1,<)}(\omega) &= -\frac{e^2}{2\pi} \mathcal{J}_{S,\perp}^2(\omega) \end{aligned} \tag{E12}$$

in the spin Kondo case, and

$$\begin{aligned} \mathbf{G}_{(1,>);(1,<)}(\omega) &= -\frac{e^2}{2\pi} \left\{ 1 - \mathcal{J}_{C,\perp}^2(\omega) \right\}, \\ \mathbf{G}_{(2,>);(1,<)}(\omega) &= \frac{e^2}{2\pi} \mathcal{J}_{C,\perp}^2(\omega) \end{aligned} \tag{E13}$$

in the charge Kondo case, with $\mathcal{J}_{S(C),\perp(z)} = \frac{aJ_{S(C),\perp(z)}}{v}$, $H_{S(C)} = -\mathcal{J}_{S(C),z}^2 + \mathcal{J}_{S(C),\perp}^2$,

$$\mathcal{J}_{S(C),\perp}(\omega) = \frac{2\sqrt{|H_{S(C)}|} \left(\frac{kT_K^{S(C)}}{\omega} \right)^{\sqrt{|H_{S(C)}|}}}{1 - \left(\frac{kT_K^{S(C)}}{\omega} \right)^{2\sqrt{|H_{S(C)}|}}}, \tag{E14}$$

and the Kondo temperature $kT_K^{S(C)} = D_0 \{ \frac{\mathcal{J}_{S(C),z}(D_0) - \sqrt{|H_{S(C)}|}}{\mathcal{J}_{S(C),z}(D_0) + \sqrt{|H_{S(C)}|}} \}$.

Equations (E12) and (E13) provide the perturbative result for the ac conductances of interest for our work. Thus, we conclude that the only relevant effect of the Kondo dynamics on the interlead ac conduction properties of the system is encoded in the dynamical impurity spin Green's functions $\mathcal{G}_{\mathrm{S;KS}}(t-t')$ and $\mathcal{G}_{\mathrm{S;KC}}(t-t')$. Indeed, typically, in problems dealing with ac transport across a Kondo-type impurity, the ac conductance is directly related to the (time derivatives of the) impurity spin Green's functions as discussed, for instance, in Ref. [85] in the context of microwave scattering at a quantum impurity in a Josephson junction array.

2. Perturbative calculation of the conductance in the disconnected lead limit

In the disconnected lead limit, the leading boundary perturbation in the lattice framework is given by H_{DL} in Eq. (30), which we adopt in the following as our perturbing boundary Hamiltonian, with the symmetric simplification $\lambda_1 = \lambda_2 = \lambda$ and with (in terms of the lattice model Hamiltonian parameters)

$$\lambda \sim \frac{t^2}{2\delta}, \quad \kappa \sim \left(\frac{t}{2\delta} \right)^4 \delta. \tag{E15}$$

(See Appendix C for details.) H_{DL} commutes with the total charge density at $x = 0$ in both leads. Therefore, the current operators defined in Eqs. (A14) are now given by

$$\begin{aligned} I_{1,<} &= ev\{\psi_{e,1}^\dagger(0)\psi_{o,1}(0) + \psi_{o,1}^\dagger(0)\psi_{e,1}(0)\}, \\ I_{2,<} &= ev\{\psi_{e,2}^\dagger(0)\psi_{o,2}(0) + \psi_{o,2}^\dagger(0)\psi_{e,2}(0)\}, \\ I_{1,>} &= -ev\{\psi_{e,1}^\dagger(0)\psi_{o,1}(0) + \psi_{o,1}^\dagger(0)\psi_{e,1}(0)\}, \\ I_{2,>} &= -ev\{\psi_{e,2}^\dagger(0)\psi_{o,2}(0) + \psi_{o,2}^\dagger(0)\psi_{e,2}(0)\}. \end{aligned} \tag{E16}$$

A first important observation arising at a first glance to Eqs. (E15) and (E16) is that, since H_{DL} only contains the $-e$ fields at $x = 0$ while $I_{a,>}$ and $I_{a,<}$ are linear in terms of $\psi_{o,a}(0)$ and $\psi_{o,a}^\dagger(0)$, one obtains the exact result that $\mathbf{G}_{(2,>);(1,<)}(\omega) = \mathbf{G}_{(1,>);(2,<)}(\omega) = 0$, at any order in κ. As for what concerns corrections to the ac conductances diagonal in the lead index, following the analysis of Appendix D, we expect a perturbative calculation in κ to provide reliable results for the ac conductance tensor. Setting $\kappa = 0$, our system traces back to the one we discuss in Appendix A, with $V_{od} = 0$, $V_d = \frac{t^2}{\delta}$. Therefore, setting $\kappa = 0$, we obtain the conductances $\mathbf{G}_{(1,>);(1,<)}^{(0)}(\omega)$, given by

$$\mathbf{G}_{(1,>);(1,<)}^{(0)}(\omega) = -\frac{e^2}{2\pi} \left[\frac{v^2\delta^2}{v^2\delta^2 + t^4} \right] \equiv -\frac{e^2}{2\pi} \cos^2(\delta_\kappa), \tag{E17}$$

with δ_κ single-fermion phase shift at the DL fixed point. To second order in κ, Eq. (E17) is corrected into

$$\mathbf{G}_{(1,>);(1,<)}(\omega) \approx -\frac{e^2}{2\pi} \left\{ \cos^2(\delta_\kappa) - \frac{8\, \cos(2\delta_\kappa)\kappa^2\omega^2}{3\pi^2 v^2} \right\}, \tag{E18}$$

that is, the result we used in the main text.

[1] J. Kondo, Prog. Theor. Phys. **32**, 37 (1964).
[2] A. C. Hewson, *The Kondo Problem to Heavy Fermions*, Cambridge Studies in Magnetism (Cambridge University Press, Cambridge, 1993).
[3] P. Nozières, J. Low Temp. Phys. **17**, 31 (1974).
[4] K. G. Wilson, Rev. Mod. Phys. **47**, 773 (1975).
[5] R. Bulla, T. A. Costi, and T. Pruschke, Rev. Mod. Phys. **80**, 395 (2008).
[6] I. Affleck and A. W. W. Ludwig, Phys. Rev. B **48**, 7297 (1993).
[7] L. P. Kouwenhoven and L. Glazman, Phys. World **14**, 33 (2001).
[8] A. Alivisatos, Science **271**, 933 (1996).
[9] L. P. Kouwenhoven and C. Marcus, Phys. World **11**, 35 (1998).
[10] D. Goldhaber-Gordon, H. Shtrikman, D. Mahalu, D. Abusch-Magder, U. Meirav, and M. A. Kastner, Nature (London) **391**, 156 (1998).
[11] S. M. Cronenwett, T. H. Oosterkamp, and L. P. Kouwenhoven, Science **281**, 540 (1998).
[12] Y. Avishai, A. Golub, and A. D. Zaikin, Phys. Rev. B **63**, 134515 (2001).
[13] M.-S. Choi, M. Lee, K. Kang, and W. Belzig, Phys. Rev. B **70**, 020502(R) (2004).
[14] G. Campagnano, D. Giuliano, A. Naddeo, and A. Tagliacozzo, Phys. C (Amsterdam) **406**, 1 (2004).
[15] S. Eggert and I. Affleck, Phys. Rev. B **46**, 10866 (1992).
[16] A. Furusaki and T. Hikihara, Phys. Rev. B **58**, 5529 (1998).
[17] D. Giuliano, D. Rossini, and A. Trombettoni, Phys. Rev. B **98**, 235164 (2018).
[18] D. Giuliano, D. Rossini, P. Sodano, and A. Trombettoni, Phys. Rev. B **87**, 035104 (2013).
[19] D. Giuliano, P. Sodano, and A. Trombettoni, Phys. Rev. A **96**, 033603 (2017).
[20] N. Laflorencie, E. S. Sørensen, and I. Affleck, J. Stat. Mech. (2008) P02007.
[21] N. Crampé and A. Trombettoni, Nucl. Phys. B **871**, 526 (2013).
[22] A. M. Tsvelik, Phys. Rev. Lett. **110**, 147202 (2013).
[23] A. M. Tsvelik and W.-G. Yin, Phys. Rev. B **88**, 144401 (2013).
[24] D. Giuliano, P. Sodano, A. Tagliacozzo, and A. Trombettoni, Nucl. Phys. B **909**, 135 (2016).
[25] D. Giuliano and P. Sodano, Nucl. Phys. B **811**, 395 (2009).
[26] A. Cirillo, M. Mancini, D. Giuliano, and P. Sodano, Nucl. Phys. B **852**, 235 (2011).
[27] D. Giuliano and P. Sodano, Europhys. Lett. **103**, 57006 (2013).
[28] B. Béri, Phys. Rev. Lett. **110**, 216803 (2013).
[29] B. Béri and N. R. Cooper, Phys. Rev. Lett. **109**, 156803 (2012).
[30] A. Altland, B. Béri, R. Egger, and A. M. Tsvelik, Phys. Rev. Lett. **113**, 076401 (2014).
[31] I. Affleck and D. Giuliano, J. Stat. Phys. **157**, 666 (2014).
[32] A. Taraphder and P. Coleman, Phys. Rev. Lett. **66**, 2814 (1991).
[33] K. A. Matveev, Phys. Rev. B **51**, 1743 (1995).
[34] G. Zaránd, G. T. Zimányi, and F. Wilhelm, Phys. Rev. B **62**, 8137 (2000).
[35] A. Buxboim and A. Schiller, Phys. Rev. B **67**, 165320 (2003).
[36] K. Le Hur, P. Simon, and L. Borda, Phys. Rev. B **69**, 045326 (2004).
[37] P. S. Cornaglia, H. Ness, and D. R. Grempel, Phys. Rev. Lett. **93**, 147201 (2004).
[38] M. Dzero and J. Schmalian, Phys. Rev. Lett. **94**, 157003 (2005).
[39] S. Andergassen, T. A. Costi, and V. Zlatić, Phys. Rev. B **84**, 241107(R) (2011).
[40] M. S. Laad, L. Craco, and A. Taraphder, Europhys. Lett. **88**, 20008 (2009).
[41] A. Furusaki and K. A. Matveev, Phys. Rev. B **52**, 16676 (1995).
[42] Z. Iftikhar, S. Jezouin, A. Anthore, U. Gennser, F. D. Parmentier, A. Cavanna, and F. Pierre, Nature (London) **526**, 233 (2015).
[43] I. Garate, Phys. Rev. B **84**, 085121 (2011).
[44] T.-F. Fang, A.-M. Guo, H.-T. Lu, H.-G. Luo, and Q.-F. Sun, Phys. Rev. B **96**, 085131 (2017).
[45] S. M. Tabatabaei, Phys. Rev. B **97**, 235131 (2018).
[46] G. E. D. K. Prawiroatmodjo, M. Leijnse, F. Trier, Y. Chen, D. V. Christensen, M. von Soosten, N. Pryds, and T. S. Jespersen, Nat. Commun. **8**, 1 (2017).
[47] A. Altland, B. Béri, R. Egger, and A. M. Tsvelik, J. Phys. A: Math. Theor. **47**, 265001 (2014).
[48] A. Altland and R. Egger, Phys. Rev. Lett. **110**, 196401 (2013).
[49] E. Eriksson, A. Nava, C. Mora, and R. Egger, Phys. Rev. B **90**, 245417 (2014).
[50] V. Mourik, K. Zuo, S. M. Frolov, S. R. Plissard, E. P. A. M. Bakkers, and L. P. Kouwenhoven, Science **336**, 1003 (2012).
[51] L. P. Rokhinson, X. Liu, and J. K. Furdyna, Nat. Phys. **8**, 795 (2012).
[52] A. Das, Y. Ronen, Y. Most, Y. Oreg, M. Heiblum, and H. Shtrikman, Nat. Phys. **8**, 887 (2012).
[53] J. Alicea, Phys. Rev. B **81**, 125318 (2010).
[54] L. Fu and C. L. Kane, Phys. Rev. Lett. **100**, 096407 (2008).
[55] R. Žitko and J. Bonča, Phys. Rev. B **74**, 224411 (2006).
[56] J. Nilsson, A. R. Akhmerov, and C. W. J. Beenakker, Phys. Rev. Lett. **101**, 120403 (2008).
[57] D. Giuliano, S. Paganelli, and L. Lepori, Phys. Rev. B **97**, 155113 (2018).
[58] I. Affleck and D. Giuliano, J. Stat. Mech. (2013) P06011.
[59] L. Fu, Phys. Rev. Lett. **104**, 056402 (2010).
[60] A. Zazunov, A. Altland, and R. Egger, New J. Phys. **16**, 015010 (2014).
[61] M. R. Galpin, A. K. Mitchell, J. Temaismithi, D. E. Logan, B. Béri, and N. R. Cooper, Phys. Rev. B **89**, 045143 (2014).
[62] A. Zazunov, A. L. Yeyati, and R. Egger, Phys. Rev. B **84**, 165440 (2011).
[63] E. Eriksson, C. Mora, A. Zazunov, and R. Egger, Phys. Rev. Lett. **113**, 076404 (2014).
[64] Y. Oreg, G. Refael, and F. von Oppen, Phys. Rev. Lett. **105**, 177002 (2010).
[65] R. M. Lutchyn, J. D. Sau, and S. Das Sarma, Phys. Rev. Lett. **105**, 077001 (2010).
[66] F. E. Di Lorenzo, The Maxwell capacitance matrix, white paper WP110301, 2011 (unpublished).
[67] R. J. Wenzel, *G-MTT International Symposium Digest* (IEEE, Piscataway, NJ, 1966), Vol. 66, pp. 94–100.
[68] M. Garst, S. Kehrein, T. Pruschke, A. Rosch, and M. Vojta, Phys. Rev. B **69**, 214413 (2004).
[69] P. W. Anderson, Phys. Rev. **124**, 41 (1961).
[70] J. Cardy, *Scaling and Renormalization in Statistical Physics*, Cambridge Lecture Notes in Physics (Cambridge University Press, Cambridge, 1996).
[71] I. Affleck, J. Phys. Soc. Jpn. **74**, 59 (2005).
[72] T. A. Costi, Phys. Rev. Lett. **85**, 1504 (2000).
[73] A. F. Otte, M. Ternes, K. von Bergmann, S. Loth, H. Brune, C. P. Lutz, C. F. Hirjibehedin, and A. J. Heinrich, Nat. Phys. **4**, 847 (2008).

[74] V. Barzykin and I. Affleck, Phys. Rev. Lett. **76**, 4959 (1996).
[75] V. Barzykin and I. Affleck, Phys. Rev. B **57**, 432 (1998).
[76] J. D. Sau, R. M. Lutchyn, S. Tewari, and S. Das Sarma, Phys. Rev. Lett. **104**, 040502 (2010).
[77] C. Wu, B. A. Bernevig, and S.-C. Zhang, Phys. Rev. Lett. **96**, 106401 (2006).
[78] C. P. Moca, I. Weymann, and G. Zarand, Phys. Rev. B **84**, 235441 (2011).
[79] P. W. Anderson and G. Yuval, Phys. Rev. Lett. **23**, 89 (1969).
[80] P. W. Anderson, G. Yuval, and D. R. Hamann, Phys. Rev. B **1**, 4464 (1970).
[81] P. W. Anderson, J. Phys. C: Solid State Phys. **3**, 2436 (1970).
[82] M. Kindermann, Phys. Rev. B **71**, 165332 (2005).
[83] Y. Tanaka, A. Furusaki, and K. A. Matveev, Phys. Rev. Lett. **106**, 236402 (2011).
[84] J. I. Väyrynen, F. Geissler, and L. I. Glazman, Phys. Rev. B **93**, 241301(R) (2016).
[85] M. Goldstein, M. H. Devoret, M. Houzet, and L. I. Glazman, Phys. Rev. Lett. **110**, 017002 (2013).